

Massive asphalt deposits, oil seepage, and gas venting support abundant chemosynthetic communities at Campeche Knolls, southern Gulf of Mexico

Heiko Sahling^{1,2*}, Christian Borowski^{2,3}, Elva Escobar-Briones⁴, Adriana Gaytán-Caballero⁴, Chieh-Wei Hsu¹, Markus Loher², Ian MacDonald⁵, Yann Marcon⁶, Thomas Pape^{1,2}, Miriam Römer^{1,2}, Maxim Rubin Blum³, Florence Schubotz², Daniel Smrzka⁷, Gunter Wegener^{2,3}, Gerhard Bohrmann^{1,2}

¹Department of Geosciences at the University of Bremen, Klagenfurter Str., 28359 Bremen, Germany

²MARUM Center for Marine Environmental Sciences, Leobener Str., 28359 Bremen, Germany

³Max-Planck Institute for Marine Microbiology, Celsiusstr. 1, 28359 Bremen, Germany

⁴Universidad Nacional Autónoma de México, Instituto de Ciencias del Mar y Limnología, A. P. 70-305 Ciudad Universitaria, 04510 Mexico City, México

⁵Florida State University, POB 3064326, Tallahassee, FL 32306, USA

⁶Alfred Wegener Institute Helmholtz Centre for Polar and Marine Research, HGF-MPG Group for Deep Sea Ecology and Technology, Am Handelshafen 12, 27570 Bremerhaven, Germany

⁷Center for Earth Sciences, University of Vienna, Althanstr. 14, 1090 Vienna, Austria

Correspondence to: H. Sahling (hsahling@marum.de)

Abstract. Hydrocarbon seepage is a widespread process at continental margins of the Gulf of Mexico. We used a multidisciplinary approach including multibeam mapping and visual seafloor observations with different underwater vehicles to study the extent and character of complex hydrocarbon seepage in the Bay of Campeche, southern Gulf of Mexico. Our observations showed that seafloor asphalt deposits previously only known from the Chapopote Knoll occur also at numerous other knolls and ridges in water depths from 1230 to 3150 m. In particular the deeper sites (Chapopote and Mictlan Knolls) were characterized by asphalt deposits accompanied by extrusion of liquid oil in form of whips or sheets, and in some places (Tsanyao Yang, Mictlan, and Chapopote Knolls) by gas emission and the presence of gas hydrates in addition. Molecular and stable carbon isotopic compositions of gaseous hydrocarbons suggest their primarily thermogenic origin. Relatively fresh asphalt structures were settled by chemosynthetic communities including bacterial mats and vestimentiferan tubeworms, whereas older flows appeared largely inert and devoid of corals and anemones at the deep sites. The gas hydrates at Tsanyao Yang and Mictlan Knolls were covered by a 5 to 10 cm thick reaction zone composed of authigenic carbonates, detritus, and microbial mats, and were densely colonized by 1–2 m long tubeworms, bivalves, snails, and shrimps. This study increased the knowledge on the occurrences and dimensions of asphalt fields and associated gas hydrates at Campeche Knolls. The extent of all discovered seepage structure areas indicates that emission of complex hydrocarbons is a widespread and, thus, important feature in the southern Gulf of Mexico.

1 **1 Introduction**

2 Asphalt volcanism in the Campeche Knolls, southern Gulf of Mexico (GoM) has been described as a distinct form of natural
3 hydrocarbon seepage (MacDonald et al., 2004). Heavy oil is extruded and forms lava-like flows that cover ~100 to ~1000 m²
4 of abyssal knolls and ridges (Brüning et al., 2010). The flows consist of high density oil with an abundant asphaltene fraction
5 (MacDonald et al., 2004) with a terpane composition similar to what has been reported from some crude oils in the Campeche
6 Sound (Scholz-Böttcher et al., 2008; Schubotz et al., 2011b). As described by Brüning et al. (2010), the heavy oil is at a
7 transition point between mobile and immobile when it flows; fluid-phase material can spread smoothly over the seafloor and,
8 because its density is initially less than seawater, local bulges and “whips” occur due to buoyancy. After exposure to seawater,
9 the heavy oil solidifies to brittle layers because of weathering processes and loss of volatile hydrocarbons. Fissures and cracks
10 through the solidified asphalt deposits were observed to develop with time. Fragmentation of brittle asphalt proceeds until
11 cobble-to-boulder sized pieces become buried by sedimentation (Brüning et al., 2010).

12 Most of the research conducted so far concentrated on the type locality, Chapopote Knoll, which was named after the Aztec
13 word for tar. Because it forms a knoll with a central crater-like depression with extensive hard substrata, the term “asphalt
14 volcano” was introduced for Chapopote Knoll (MacDonald et al., 2004). Chapopote Knoll is suggested to overlie a reservoir-
15 seal system for hydrocarbons. From seismic studies it was inferred that coarse-grained sediments sealed by a thin (100-200 m)
16 veneer of fine-grained sediments within the core of the knoll act as temporal hydrocarbon reservoir (Ding et al., 2008). Ding
17 et al. (2008) speculated that the shallow reservoir plays a role in creating a heavy oil prior to its seafloor discharge: The oil in
18 the region forms from Jurassic source material that has solidified within the hydrocarbon generation window over extended
19 time (Magoon et al., 2001). Processes such as biodegradation, water washing or gas injection in the shallow reservoir could
20 further increase its specific gravity (Tissot and Welte, 1984). However, Schubotz et al. (2011b) did not find evidence for
21 biodegradation in ductile (fresh) asphalts, so the sequence leading to the characteristic asphalt deposition remains speculative.
22 In Campeche Knolls, oil seepage is widespread as evidenced by sea surface oil slicks detected by synthetic aperture radar
23 satellite images (Fig.1; Williams et al., 2006). The sea surface slicks occur above dozens of knolls and ridges (Ding et al.,
24 2010) and are thus, a significant component of natural seepage in the southwestern Gulf of Mexico (MacDonald et al. 2015).
25 Seismic studies at the knolls and ridges indicate shallow sub-surface hydrocarbon accumulation as well (Ding et al., 2010) but
26 prior to the present study it was unclear whether these systems also produced asphalt deposits at the seafloor.

27 The natural hydrocarbon seeps at Chapopote Knoll comprise typical seep components that provide habitat for diverse
28 biological communities. For example, in addition to asphalt deposits, there are reports of oil-soaked sediments (MacDonald et
29 al., 2004; Schubotz et al., 2011a, b), gas hydrate occurrences (MacDonald et al., 2004, Schubotz et al., 2011b, Klapp et al.,
30 2010a, b), gas venting (Brüning et al., 2010), and authigenic carbonates (Naehr et al., 2009). The asphalt deposits sustain
31 hydrocarbon-degrading and sulfate-reducing bacteria within their interior (Schubotz et al., 2011b), surface bacterial mats, and
32 vestimentiferan tubeworms that colonize fissures in the asphalt deposits (MacDonald et al., 2004; Brüning et al., 2010). Oil-
33 impregnated sediments were found to harbor a complex microbial community that sustained both methanotrophy and

1 methanogenesis (Schubotz et al., 2010a, b). The stable isotopes of methane in gas hydrates associated with asphalt suggested
2 methanogenesis (Schubotz et al., 2011b). Two species of mytilid mussel (*Bathymodiolus brooksi* and *B. haeckeri*) occurred
3 close to an oil and gas seep, harboring different endosymbiotic communities (Raggi et al., 2013). A novel symbiont related to
4 the hydrocarbon-degrading bacteria genus *Cycloclasticus* was verified in the seep-associated mussel *B. heckerae* (Raggi et al.,
5 2013).

6 Subsequent to the initial discovery at Chapopote Knoll (MacDonald et al., 2004) asphalt deposits were found at other
7 continental margin settings as well. In the Santa Barbara Basin off California, asphalt volcanoes about 15 and 20 m high
8 formed 31 to 44 kyr ago (Valentine et al., 2010). These structures occur at water depths of around 150 to 180 m in a region
9 additionally comprising tar mounds at ~30 m depths (Vernon and Slater, 1963). In the northern Gulf of Mexico, asphalt mounds
10 about one meter in height and up to several meters in basal diameter exist in the Puma Appraisal Area (Weiland et al., 2008)
11 and the Shenzi Field (Williamson et al., 2008) at water depths of about 1500 m. In addition, more than 2000 asphalt mounds
12 with diameter ranging from less than a meter up to 50 m in diameter were observed on the Angolan margin at water depth
13 between 1350 and 2150 m (Jones et al., 2014). Based on their morphological appearance, their partial coverage by sediments,
14 and the general lack of chemosynthetic organisms growing on the asphalt, the asphalt deposits in other regions seem to be
15 older than those described in the southern GoM (Brüning et al., 2010). Moreover, in contrast to those in the southern GoM,
16 asphalt deposits in the other regions are populated by regular, heterotrophic deep-sea organisms growing on hard substrate.
17 Old asphalt deposits have, therefore, been suggested to foster the deep-sea habitat heterogeneity and provide additional settling
18 grounds for species dispersal, which results in an increase in overall diversity (Jones et al., 2014). The Campeche Knoll asphalt
19 region remains the deepest example known to date. The potential influence of pressure and temperature on emission of asphalt,
20 liquid oil, and gas, and their interaction with microbial and metazoan communities, warrants further investigations.

21 We conducted an interdisciplinary research campaign to the Campeche Knolls in spring 2015 on board the research vessel
22 *Meteor*. Sites for investigation were developed following a nested approach. We used the information of oil slicks at the sea
23 surface (Williams et al., 2006; MacDonald et al. 2015; Suresh 2015) to systematically identify potential targets with active
24 hydrocarbon systems. To further focus our activities, we looked for evidence of gas bubble emissions by scanning the water
25 column with ship-based hull-mounted multibeam echosounder. High-resolution bathymetry of the most promising sites was
26 acquired by the SEAL 5000 autonomous underwater vehicle (AUV) mapping. Finally, we conducted seafloor observations
27 and sampling by QUEST 4000m remotely operated vehicle (ROV), concentrating on three sites at depths > 2900m.
28 Specifically, we were interested in disentangling the various seafloor manifestations resulting from the geochemically diverse
29 seepage of heavy oil (leading to asphalt deposits), oil (leading to sea surface slicks) and gas (as bubbles and hydrate deposits).
30 By concentrating on the description of the different environments that we encountered at the hydrocarbon seeps, we provide
31 an overview for more detailed studies that will focus on the geochemistry of different oils, authigenic carbonate composition,
32 microbiology, and fauna. We additionally show, based on our recent findings and results obtained during three precursor
33 cruises (Bohrmann and Schenk, 2004; Bohrmann et al., 2008; MacDonald et al., 2007), that asphalt deposits are not limited to
34 the type locality Chapopote Knoll, but are inherent to natural hydrocarbon seepage in the entire Campeche Knolls.

1 **2. Geological Setting of Campeche Knolls**

2 Campeche Knolls (Fig. 1) is part of the large South Gulf Salt Province that stretches from the southern land margin across the
3 shelf and Campeche Knolls to Sigsbee Knolls in the north. The Sigsbee Abyssal Plain separates the salt province in the southern
4 GoM from the Mississippi-Texas-Louisiana salt province in the north. Salt tectonism in the southern deep GoM basin is
5 believed to be an analogue to that of the Texas–Louisiana slope (Garrison and Martin, 1973). Because the basins share similar
6 salt deposition histories, it is inferred that most of the salt was deposited during the rifting stage of the Gulf in the Late Jurassic,
7 equivalent to the Louann salt of the Texas–Louisiana slope (Salvador, 1991).

8 Campeche Knolls comprise knolls and ridges that are limited to the west by smooth abyssal seafloor of the salt-free Veracruz
9 tongue (Bryant et al., 1991). The Campeche Canyon, which is not a canyon in erosional sense, formed through the development
10 of the eastern limit of Campeche Knolls and the carbonate Campeche Platform. Northward, smooth seafloor separates the
11 Campeche Knolls from the Sigsbee Knolls. The Campeche Knolls is covered by a 5-10 km sediment column that hosts prolific
12 petroleum source rocks, with the most productive being of latest Jurassic and Cretaceous age (Magoon et al., 2001). Most of
13 the sediment thickness results from deposition during Cenozoic times and was controlled by orogenic events in the Mexican
14 region and sea-level changes.

15 The distribution of oil slicks at the sea surface (Williams et al., 2006; MacDonald et al., 2015; Suresh, 2015) aggregates along
16 the northwestern sector of the Campeche Knolls (Fig. 1). Interpretation of seismic lines and basin modeling carried out by the
17 Mexican petroleum company PEMEX led to the conclusion that the sub-province designated as 4S (Fig. 1) contains the largest
18 allochthonous and autochthonous salt deposits (Cruz-Mercado et al., 2011; Sánchez-Rivera et al., 2011). The actual density of
19 salt bodies increases from southeast to the northwestern region of Campeche Knolls. It is proposed that gravitational forces
20 toward the northwest cause contraction and compression in the northwestern distal part of the system in which structural folds,
21 high-angle reverse faults and numerous allochthonous salt bodies developed since the late Miocene to Recent (Cruz-Mercado
22 et al., 2011; Sánchez-Rivera et al., 2011).

23 **3 Material and Methods**

24 Natural oil slicks at the sea surface were detected by synthetic aperture radar in the region of the southern GoM by Williams
25 et al. (2006). Based on their analyses of repeated observations, they postulated seep locations on the seafloor that could be the
26 origins of the oil slicks. With regard to interpretation limits of the remotely sensed data they distinguished between definite,
27 probable and possible seep locations. Figures 1 and 2 show the inferred seep locations they classified as definite or probable.
28 We excluded the numerous possible seep locations for clarity and also because many of the possible seeps were located outside
29 of Campeche Knolls, suggesting that the corresponding oil slicks might not be caused by natural oil seepage. Those sea surface
30 patterns might have been caused by other processes, i.e. algae blooms, local wind fields, or anthropogenic activity.

1 Ship-based hydroacoustic surveys, and dives with an autonomous underwater vehicle (AUV) and a remotely-operated vehicle
2 (ROV) were conducted during cruise R/V *Meteor* (M 114) 12 February to 28 March 2015.

3 The multibeam echosounder (MBES) Kongsberg EM122 operating at 12 kHz was used for bathymetric mapping. Together
4 with bathymetry data collected during two earlier cruises with R/V *Sonne* in 2003 (SO 174; Bohrmann and Schenk, 2004) and
5 R/V *Meteor* (M67/2; Bohrmann et al., 2008) good bathymetric coverage was acquired in the entire northwestern sector of the
6 Campeche Knolls (Fig. 2).

7 We additionally examined the water column data of the MBES systematically for evidence of gas emissions along the entire
8 cruise track of M 114 (Fig. 2, inset). Water column imaging for the detection of gas bubble plumes was conducted with the
9 Fledermaus Midwater software program (company: Quality Positioning Services B. V., The Netherlands). Gas bubble plumes
10 cause high backscatter in the water column. In this paper we assume that all acoustic anomalies were related to gas venting
11 and will refer to them as “flares”. Flares were traced through the water column by analyzing swath by swath, which results in
12 a three dimensional representation of the bubble streams. We detected numerous gas bubble flares, of which some could be
13 traced completely from the water column down to the seabed. Most flares, however, were only observed in the mid-water
14 column and the point of origin at the seabed could not be traced. In those instances, we projected the flares down to the seafloor
15 and give this point as coordinates. We assume that this lack of backscatter from gas bubbles in great water depths results from
16 the pressure dependence of the backscatter strength (Greinert et al., 2006). Further in-depth studies are required to confirm
17 this. For the objectives of this study, we linearly projected flares from mid-water depths to the seabed and assumed that bubbles
18 were escaping the seafloor around these sites. We defined surveys areas at the seafloor that included the putative gas emission
19 sites and conducted AUV-based micro-bathymetric mapping and ROV-mounted horizontally scanning sonar to locate gas
20 emission sites.

21 High-resolution bathymetry data were acquired with the MBES Kongsberg 2040 during dives with the AUV SEAL 5000 at
22 an altitude of 80 m. Ship-based and AUV-based bathymetry data were processed with MB-Systems (Caress and Cheyes, 2014).
23 The Kongsberg 675 kHz Type 1071 forward-looking sonar on ROV QUEST 4000m was used for the localization of bubble
24 plumes following the method described in Nikolovska et al. (2008). Seafloor images shown in this study were taken either
25 with the digital Inside Pacific Scorpio 3.3 mega-pixel still camera or frame-grabbed (Adobe Premiere Pro) from video footage
26 gained with the Insite Pacific Zeus 3CCD HDTV video camera.

27 In order to characterize geochemically the different hydrocarbon components, gas bubbles (clear and oil-coated) and oil drops
28 released from the seafloor were captured with the pressure-tight Gas Bubble Sampler (GBS) at four different knolls and ridges
29 (Supplementary Table 1). Two bubble streams were sampled at Tsanyao Yang Knoll whereas at all other sites investigated
30 only one bubble stream was sampled. Gas bubble samples were not recovered from Knoll 2000. Repeated sampling was
31 conducted at Mictlan Knoll during different dives and at different heights above the seafloor. Oil drops were captured together
32 with chimney-like structures at Marker M114-5 at a site similar in appearance to that shown in Fig. 6 D. The samples were
33 analyzed for molecular compositions and $\delta^{13}\text{C}\text{-CH}_4$ signatures according to Pape et al. (2010) and Römer et al. (2012).
34 Biological samples were taken by push corer, scoop net, manipulator, or baited trap with the help of the ROV. Based on the

1 video footage and studies of the animals on board, we identified the fauna to various taxonomic levels but detailed on-shore
2 studies are needed to fully explore their taxonomy.
3 Underwater navigation of AUV and ROV were achieved by use of the Ixsea Posidonia ultra short baseline system. Spatial data
4 were integrated into the Arc-GIS program (ESRI) and maps were produced by combined usage of the Arc-GIS and Adobe
5 Illustrator programs.
6 Camera sled surveys were conducted during cruises SO 174 (Bohrmann and Schenk, 2004), M 67/2 (Bohrmann et al., 2008),
7 and “Chapopote III” with R/V *Justo Sierra* in 2007 (MacDonald et al., 2007). Three different camera systems were used for
8 taking video images (M 67/2 and Chapopote III) and photographs (SO 174) at the seafloor. The locations of camera sled
9 observations given in Table 1 are approximated based on ship position.

10 **4 Results**

11 **4.1 Site descriptions**

12 **4.1.1 Tsanyao Yang Knoll (about 3400 m water depth)**

13 Tsanyao Yang Knoll is a dome approximately 400 m high and 6 km wide (Fig. 3 A), which we named after Prof. Tsanyao
14 Yang from the Department of Geosciences, National University of Taiwan. “Frank” Yang dedicated his life to study mud
15 volcanoes and hydrocarbon seeps on- and offshore Taiwan; he sadly passed away while we were conducting this present study
16 at sea.

17 Gas emissions were recorded as flares with the echosounder from the seafloor at water depths as great as to 3500 m at the
18 plateau-like summit (Fig. 3 A). Figure 3 B shows the ROV dive track within a depression about 150 to 200 m wide and 30 m
19 deep. Here, we discovered spectacular gas-hydrate exposures at three sites (Site 1, 2, and 3) at depths of about 3420 m. In
20 contrast to the knolls and ridges further south, we did not observe during the dives wide-spread asphalt deposits at Tsanyao
21 Yang Knoll.

22 The gas hydrates were found in mounds that were 1-2 m high and 3-10 m wide at their bases and that were densely colonized
23 by vestimentiferan tubeworms probably of the genus *Escarpia* (Fig. 4 A). The mounds had regular borders of gravel- to
24 boulder-sized rock clasts and shells that separated seep-influenced from normal deep-sea sediments. In some locations, clusters
25 of living vesicomimid clams (*Abyssogena southwardae*) were observed in the transition zone. In several instances, the mounds
26 were fractured, exposing 1-2 m hanging walls of gas hydrate with vigorous gas bubble streams observed emitting from the
27 base (Fig. 4 B). Exposed hydrate preserved a fabric of frozen bubbles, which indicated rapid formation (Suess et al., 2001).
28 Some bubble-fabric gas hydrate formed from rising bubbles when they attached to the vertical wall due to adhesion or were
29 captured by overhanging structures. Many bubble streams were composed of transparent bubbles forming white gas hydrates
30 but some streams contained oil-coated bubbles forming blackish-colored hydrates. We additionally observed dense hydrate

1 cropping out over most of the visible exposed fracture, as exemplified in Fig. 4 B. Most of the hydrate was white, but blackish-
2 stained hydrate was also observed.

3 The outermost 5 to 10 cm thick layer of the mounds were composed of authigenic carbonates entangled with the posterior parts
4 of the vestimentiferan tubes and other detritus. For convenience, we term these tubeworm parts the “rhizosphere” hereafter.
5 Fleshy, thick microbial mats were attached to the carbonates in the lower portion of the rhizosphere. We hypothesize that the
6 carbonates were formed under anoxic conditions in the interior of the rhizosphere, similar to those authigenic carbonates
7 growing in the sediments within the sulfate-methane transition zone at other seeps (Formolo et al., 2004). A flourishing
8 ecosystem of seep-typical fauna (e.g. living mytilid mussels, gastropods, *Alvinocaris* sp. shrimp) occupied the top of the
9 carbonates at the base of the vestimentiferan tubes (Fig. 4 C). The vestimentiferan tubes were densely overgrown by colonies
10 of epifaunal suspension feeders (e.g. hydrozoans and anemones).

11 At site 3, we observed a mound composed of reworked sediment components and gravel to pebble-sized rocks (Fig. 4 D). An
12 exposed lens-shaped chunk of hydrate (1.5 m wide and 0.5 m high) was present at the top of the mound (Fig. 4 E). The upper
13 part of the hydrate showed a dense fabric while the lower part was porous suggesting that it formed from frozen gas bubbles
14 (Fig. 4 F). The two hydrate fabrics were separated by a layer that looked like organic material. Ice worms (cf. *Hesiocaeca*
15 *methanicola*) were observed living in the bubble-fabric hydrate.

16 **4.1.2 Mictlan Knoll (about 3100 m water depth)**

17 Mictlan Knoll features the characteristics of an asphalt volcano (sensu MacDonald et al., 2004) with a crater-like summit area
18 on top of an approximately 250 m high circular knoll that is about 10 km wide at its base (Fig. 5 A). This knoll contained
19 diverse and widespread structures related to heavy oil seepage. We named it Mictlan, which means underworld in the Aztec
20 language.

21 The MBES surveys revealed evidence for gas emission along the crater rim. We conducted five ROV dives on different areas
22 of the crestal region (Fig. 5 B) and illustrate our findings with images from four sites: Hydrate Hill, Marker M114-5, Marker
23 M114-1, and “fresh asphalts”.

24 Hydrate Hill is a 30 m high elevation with a densely populated vestimentiferan tubeworm field (c.f. *Escarpia* spp.) on its top
25 that was 20 to 30 m wide (Fig. 6 A-C). At the summit, gas escaped the seafloor and gas hydrates occurred below an overhanging
26 protrusion consisting of carbonates and vestimentifera. Exposed rocks at the base of the hill appeared to be fragmented asphalts
27 (Fig. 6 C) but no samples were recovered. We therefore suggest that the entire hill is an accumulation of asphalt talus that is
28 covered at its summit by authigenic carbonates and vestimentifera.

29 At Marker M114-5, we observed 1-2 m sized asphalt humps with small colonies of vestimentiferan tubeworms that were less
30 than one meter long. Remarkably, at this site viscous oil was slowly seeping (about one drop every few minutes) through
31 slender, white-coated chimneys some 10 to 30 cm in height (Fig. 6 D). In the area around Marker M114-5 about 10 sites with
32 chimney clusters were observed.

1 At Marker M114-1, oil seepage occurred through a flat-topped mound about 1 m high and tens of meters wide, which was
2 composed of fragmented asphalt and soft sediments. The mound surface was covered by a highly patchy community of 50 cm
3 long vestimentiferan tubeworms, mytilid bivalves (*Bathymodolus brooksi*), bacterial mats, and various epizoic groups of
4 suspension feeders such as sponges, hydrozoa, and anemones (Fig. 6 E, F). Oil drops escaped the sediments at a low rate (one
5 drop of oil every 1-5 minutes). Rising drops remained at first attached to the seafloor by elongating threads and only eventually
6 broke loose, leaving behind strands of oil that floated or adhered to the nearby organisms. Oil was released from the sediments
7 also during sampling of sediments and organisms collected with the ROV and the sample material was heavily soaked with
8 oil when recovered aboard ship.

9 In the area denoted as “fresh asphalts” (Fig. 5B) we observed a variety of structures that provide insight into the flow behavior
10 of heavy oil deposition at the seafloor. Although the extrusion process of heavy oil was not directly observed by us at the
11 seafloor, the resulting flow structures are illustrative. Based on our observations, two main types of heavy-oil emission and
12 post-emission behavior may be distinguished. The first type includes extrusion of heavy oil forming strands or sheets that float
13 into the water due to positive buoyancy while they remain attached to the seabed owing to cohesion (Fig. 7 A-C). Over time,
14 the strands and sheets apparently lose buoyancy and pile up on the seafloor forming decimeter to meter-high accumulations.
15 The second type comprises extrusion of oil that is heavier than seawater and spreads on the seabed following gravity (Fig. 7
16 D-F). These flows solidify over time and, subsequently, accumulate sediments on their surface as illustrated in Figs. 7 E and
17 F. Dimensions of flows observed in this study ranged between decimeter and tens of meters in diameter.

18 **4.1.3 Chapopote Knoll (about 2900 m water depth)**

19 Flare mapping with the ship-based MBES system revealed that plumes interpreted to be due to gas emission at this site were
20 widespread along the crater rim (Fig. 8 A). Flares were rather dispersed; consequently, we mapped areas with gas emissions
21 rather than individual emission sites. Subsequent ROV dives focused on the 50 m wide flow of the main asphalt field and a
22 location that had been named the “bubble site” during previous visits (Fig. 8 B; Brüning et al., 2010).

23 First analysis of results obtained during our return visit in 2015 revealed that the appearance of the main asphalt field was little
24 altered from what was observed during the first exploration in 2006 (Brüning et al. 2010). The extent of the flow and
25 distributions of bacterial mats and vestimentiferan tubeworm remained largely unchanged. While expanding the mapped area
26 in the course of this study, it became apparent that the main asphalt flows terminated on soft sediments in the north and west
27 (Fig. 9 A), but overlaid older flows characterized by fragmented asphalts (Fig. 9 B) toward the south and east. Noting
28 significant sediment cover on older asphalts, we conjecture that the main asphalt flow represents the most recent stage of
29 several flow events.

30 The “bubble site” is located on a ridge several meters high that is formed of fragmented asphalts with soft sediments
31 interspersed between the flow breccia. Gas bubbles escaped the seafloor and gas hydrates were present below a seafloor
32 protrusion (Fig. 9 C, D). Recovered sediments and rocks were heavily impregnated with oil. The fauna comprised mytilid

1 bivalves including *Bathymodiolus heckerae*, *B. brooksii*, vestimentiferan tubeworms, and a variety of organisms attracted by
2 the seep system, such as *Munidopsis geyeri* and *Alvinocaris muricola* crustaceans (Gaytán-Caballero, 2009), gastropods and
3 sponges (Fig. 9 D, E). A few meters away from the “bubble site”, oil drops or oil-coated bubbles were released from the
4 seafloor (Fig. 9 F) and dark orange, oil coated hydrate masses were exposed.

5 **4.1.4 Knoll 2000 (about 1850 m water depth)**

6 Knoll 2000 is an elongated feature next to a ridge with two faint flares that originated on the eastern flank of the knoll (Fig.
7 10). During an ROV dive authigenic carbonates and dark-stained sediments with whitish patches, interpreted to be bacterial
8 mats, were observed (Fig. 11 E, F). Some of the authigenic carbonates were dark-stained and may contained asphalt. The
9 recovery of frenulate tubeworms (Siboglinidae; Frenulata) in whitish-stained sediments (Fig. 11 E) was noteworthy because
10 species of this group were not observed at the other sites investigated in this study. However, because of their thin tubes, the
11 tubeworms were invisible for the camera systems during the dive. Gas bubble emissions were not observed during the one
12 ROV dive to Knoll 2000.

13 **4.1.5 UNAM Ridge (about 1230 m water depth)**

14 UNAM ridge is an approximately 500 m high ridge named after the *Universidad Nacional Autónoma de México* in appreciation
15 of the collaborative effort to study the deep-water hydrocarbon seeps off Mexico. This was the shallowest site visited during
16 this study. At least five flares were detected above the crest (Fig. 10). Two ROV dives revealed evidence for an active, albeit
17 senescent seep system. Remarkably, soft corals and other hard-ground suspension feeders were found to settle on
18 iron/manganese-stained carbonates and weathered asphalts (Fig. 11 A). The occurrence of vestimentiferans tubeworms was
19 limited to a few bushes. Recumbent tubeworms were dominant (Fig. 11 B), which is generally considered as an indicator for
20 a senescent community. Iron/manganese-stained carbonates were observed along with debris of mytilid shells (Fig. 11 C). The
21 most active seep site was situated on the side of a pockmark-like depression and comprised a relatively small bubble stream
22 with only few specimens of living mytilid mussels on carbonates (Fig. 11 D). On a small 20 cm high and 1 m wide sediment
23 mound we observed a white, hydrate-like texture through a drape of sediment suggesting the presence of gas hydrates but as
24 we did not attempt any sampling, we cannot prove the occurrence of hydrates.

25 **4.2 Seafloor observations by camera sled**

26 In addition to the findings during M 114, camera sled deployments during the preceding cruises SO 174, M 67/2, and
27 “Chapopote III” revealed evidence for the presence of asphalts and chemosynthetic communities at seven further knolls and
28 ridges as summarized in Table 1 and Figure 2). We realized that the identification of asphalts on the basis of images alone is

1 ambiguous because the appearance of iron/manganese-stained carbonates is similar to that of weathered asphalts as shown in
2 Figs. 11 A, C and Fig. 9 B, respectively. Nevertheless, the camera sled observations suggests that natural hydrocarbon seepage
3 is widespread in the area of the Campeche Knolls.

4 **4.3 Gas composition and isotopes**

5 Hydrocarbons analyzed from all gas bubble samples collected with the Gas Bubble Sampler from Tsanyao Yang Knoll, Mictlan
6 Knoll, Chapopote Knoll, and UNAM Ridge were dominated by methane with a C_1/C_2 -ratio varying between 14 and 185 (Fig.
7 12), the methane stable carbon isotope composition ($\delta^{13}C\text{-CH}_4$) ranged between -45.1 and -49.8‰ V-PDB. The oil drop sample
8 revealed a relative CH_4 -depletion ($C_1/C_2 = 2$) compared to the gas samples and the $\delta^{13}C\text{-CH}_4$ value (-56.4‰ V-PDB) was more
9 negative.

10 **5 Discussion**

11 **5.1 Natural hydrocarbon seepage in the Campeche Knolls**

12 The region of Campeche Knolls shows evidence of abundant natural hydrocarbon seepage. This was already evident by the
13 widespread presence of oil slicks at the sea surface (Williams et al., 2006, MacDonald et al., 2015, Suresh, 2015). Knolls and
14 ridges in Campeche Knolls are generally the seabed expressions of salt diapirism that causes hydrocarbons to accumulate and,
15 eventually, to migrate through the sediments to the seafloor (Ding et al., 2008; 2010). More than 50 knolls and ridges in our
16 study area exhibited single or multiple oil slick origins (Fig. 2), which suggests that it is as prolific natural an oil seepage area
17 as the salt province in the much better studied northern Gulf of Mexico (GoM; e.g. MacDonald et al., 1993; 1996). In Campeche
18 Knolls, hydrocarbon seepage occurs in water depths down to about 3500 m, which is considerably deeper than seeps discovered
19 at the middle-lower continental slope in the northern GoM (~2750 to ~970 m; Roberts et al., 2010). Only the seeps at the
20 Florida Escarpment are located in comparable water depths at 3300 m (Paull et al., 1984; Cordes et al., 2007b).

21 While previous studies focused on Chapopote Knoll, we summarize in this study hydrocarbon seepage at the seafloor at five
22 sites by ROV observations (including Chapopote Knoll) and, in addition, at seven sites by camera sled surveys at knolls and
23 ridges (Fig. 2, Table 1). These sites range from depths around 1100 m in the south to 3420 m in the north of the study area. At
24 all twelve sites we found evidence of natural hydrocarbon seepage as indicated by the presence of chemoautotrophic
25 communities, authigenic carbonates, or asphalt deposits, confirming that hydrocarbon seepage is a widespread process in the
26 region of Campeche Knolls. All of the twelve sites are located at the seafloor below sea surface oil slicks detected by satellite
27 imagery (Williams et al., 2006). However, it should be noted that we only studied the seafloor close to oil slicks and that our
28 method is biased, i.e. it does not provide a correlation between sea surface slicks and seafloor seepage.

1 Asphalt deposits were visually identified at seven sites (UNAM Ridge, Chapopote Knoll and Mictlan Knoll; Sites 1, 3, 6, and
2 7; Table 1) and they probably also occur at four more sites (Knoll 2000, Site 2, 4, and 5; Table 1). This clearly shows that
3 seepage of heavy oil is an intrinsic property of Campeche Knolls (Fig. 2). A possible reason for this is that the crude oil in the
4 Campeche salt province is generally heavy (Magoon et al., 2001) in terms of API gravity (American Petroleum Institute
5 gravity). For now we can only speculate on the mechanisms that lead to the expulsion and deposition of heavy oil on the
6 seafloor, but we assume it is a combination of salt tectonic movements and high gas content that lead to the rise of this heavy
7 oil to the seafloor, where it is then subjected to postdepositional weathering processes.

8 Out of the about ten sites with asphalt deposits at the seafloor, only three knolls (Chapopote Knoll, Mictlan Knoll, and Site 3;
9 Table 1) exhibit features characteristic of “asphalt volcanism” (sensu MacDonald et al., 2004) that forms conical mounts with
10 crater-like depressions and extensive hard substrata. The other sites either form ridges or the asphalts are associated with more
11 complex morphologies. Tsanyao Yang Knoll is a noteworthy exception, because we did not find indications for the presence
12 of extensive asphalt deposits, although seepage of oil was observed. The fact that we did not observe large asphalt deposits
13 might be the result of too limited survey effort. Alternatively, we speculate that the absence of asphalt deposits at Tsanyao
14 Yang Knoll are related to its unique shape as it is the only flat-topped knoll analyzed in this study: Its morphology resembles
15 that of “passive type” salt diapirs (Ding et al., 2010), where salt intruding very close to the seafloor caused bending up of
16 hydrocarbon-bearing strata to the seabed. The structural framework of passive type salt diapirs may not provide the necessary
17 shallow hydrocarbon reservoir typical for the other knolls and ridges (Ding et al., 2008; 2010).

18 During our investigations it became clear that in most instances gas venting, oil seepage, and flows of heavy oil (leading to
19 asphalt deposits) were temporally and spatially segregated. Oil and gas seepage occurred separated from asphalt occurrences
20 (e.g. at Mictlan Knoll) but also through fractures in asphalts that probably act as conduits for gas/oil migration (e.g. at Hydrate
21 Hill, Marker M114-5, Marker M114-1, and the “bubble site” at Chapopote). Different chemical compositions of oil and gas
22 result in different manifestations at the seafloor that we discuss in the following section.

23 **5.2 Geochemical characterization of gas, hydrate and oil**

24 In order to characterize the origin of hydrocarbons generated in the deep subsurface below the emission sites, we analyzed
25 bubble-forming gas escaping the seafloor. Compared to the other hydrocarbon-containing organic substances discharged at the
26 Campeche Knolls (e.g. oil, heavy oil), rapidly emitted vent gas is believed to be less affected by alteration in the course of
27 upward migration in the sediment and, thus, can provide insight into the chemical characteristics of the subsurface reservoir
28 of light hydrocarbons. Considering the molecular compositions of light hydrocarbons (expressed as C_1/C_2 -ratios) and stable
29 carbon isotopic signatures of methane ($\delta^{13}C-CH_4$) most samples plot within or close to the empirical field proposed for a
30 thermocatalytic origin (Fig. 12).

31 The variability of $\delta^{13}C-CH_4$ values in gas bubbles was noticeably small ($\Delta\delta^{13}C-CH_4 = 4.7 \text{ ‰V-PDB}$), given the fact that
32 sampling was conducted at four different knolls and ridges positioned some tens to hundreds of kilometers distant to each

1 other. In contrast, C_1/C_2 -ratios appear to be more variable with highest values determined for apparently pure gas bubbles from
2 Hydrate Hill at Mictlan Knoll (185, GeoB19336-15) and lowest values for oil-coated bubbles at Tsanyao Yang Knoll (14,
3 GeoB19337-2). A variety of possible post-genetic processes can affect the distributions of light hydrocarbons, e.g., abiotic
4 molecular fractionation during migration (Leythaeuser et al., 1980), admixture with oil-derived components or secondary
5 methane (Milkov and Dzou, 2007), and microbial oxidation of methane and non-methane hydrocarbons (Hoehler et al., 1994;
6 Joye et al., 2004; Kniemeyer et al., 2007). However, the causes for the variations in C_1/C_2 -ratios observed in this study remain
7 unexplained.

8 Methane in the gas bubbles sampled during this study was enriched in ^{13}C relative to that in oil samples ($\delta^{13}\text{C-CH}_4 < -50.3\text{‰}$),
9 which were either collected during this study (one sample) or in the course of previous studies (Fig. 12; MacDonald et al.,
10 2004; Schubotz et al., 2011b). The variability in the $\delta^{13}\text{C-CH}_4$ and C_1/C_2 -ratios of the oil samples either reflects site-specific
11 properties of the oil source or indicates alteration processes during migration to variable extents. More negative values $\delta^{13}\text{C-CH}_4$
12 of the oil samples in general may result from admixture by microbial produced ^{13}C -depleted secondary methane from the
13 oxidation of higher short-chained hydrocarbons at shallow sediment depth (Milkov and Dzou, 2007; Schubotz et al., 2011b).
14 We failed to sample gas hydrates during this study, but shallow hydrates were collected from two sites at Chapopote Knoll
15 during previous investigations (MacDonald et al., 2004; Schubotz et al., 2011b). Hydrate-bound methane in these studies was
16 depleted in ^{13}C by $> 3\text{‰}$ compared to methane in bubbles collected in our study. It should be stressed, that sampling was
17 conducted in different years and not at exactly the same sites. Nevertheless, $\delta^{13}\text{C-CH}_4$ differences between gas bubbles and
18 hydrates within Chapopote Knoll are an interesting result, as hydrate deposits close to the seafloor are considered to form from
19 gas bubbles (see below) without significant isotopic fractionation of methane (Bourry et al., 2009; Pape et al., 2010; Sassen et
20 al., 2004). The difference in $\delta^{13}\text{C}$ of $> 3\text{‰}$ between methane in bubble streams and in shallow hydrates at Chapopote Knoll,
21 therefore, suggests some contribution of microbial-generated methane to the hydrate.

22

23 **5.3 Gas venting, hydrate occurrence, and the vestimentifera-gas/hydrate habitat**

24 Gas emissions are integral parts of submarine seep systems in various geological settings worldwide but hydrate-containing
25 mounds overgrown by dense vestimentiferan tubeworm fields probably belonging to the genus *Escarpia* are, to our knowledge,
26 unique to Campeche Knolls. Massive hydrate deposits close to the seafloor are considered to result from gas bubble migration
27 through the sediments (Haeckel et al., 2004; Smith et al., 2014): Part of the gas can be sequestered as gas hydrate at shallow
28 sediment depths, in case the crystallization force overcomes the effective overburden stress (Torres et al., 2004). Shallow
29 hydrate deposits typically form a mounded topography of soft sediment at the seafloor as observed at Hydrate Ridge (Cascadia
30 Margin; Suess et al., 2001; Sahling et al., 2002) and Bush Hill in the northern GoM (MacDonald et al., 1994). At Hydrate
31 Ridge, intensive anaerobic oxidation of methane (AOM) in sediments overlying hydrates results in production of hydrogen
32 sulfide that is consumed by sulfide-oxidizing bacteria that form mats draping the mounds (Boetius et al., 2000; Treude et al.,
33 2003). Sulfate reduction coupled to the degradation of higher-order hydrocarbons brought along with oil propagating in the
34 sediments was additionally proposed to occur in the northern GoM (Formolo et al., 2004; Joye et al., 2004).

1 In our study, we found vestimentiferan tubeworms capping hydrate deposits, which has not been observed before in such a
2 clear association. In order to illustrate the relevant processes, we illustrate the two different situations encountered at Tsanyao
3 Yang Knoll and Mictlan Knoll in Fig. 13. At both knolls, gas bubbles percolated through the mounds and we propose that
4 continuous gas supply from below drives hydrate formation in the shallow sub-surface. At Tsanyao Yang Knoll, hydrate
5 formed as massive layers in the sediments within the mound (Fig. 4 B) whereas for Mictlan Knoll we speculate that hydrates
6 occupy voids between fragmented asphalt (Fig. 6 A-C). In both cases, hydrates serve as methane reservoir (e.g. Sahling et al.,
7 2002) from which methane and other short-chained hydrocarbons are constantly diffusing towards the overlying seawater.
8 We further propose that AOM dominates in the rhizosphere which is a distinct 5-10 cm thick layer consisting of the posterior
9 tubes of the vestimentiferan tubeworms. Vestimentiferan tubeworms can release sulfate through their posterior tubes
10 (Dattagupta et al., 2006, 2008) and we therefore suggest that the rhizosphere in particular is supporting AOM. Due to the fact
11 that AOM efficiently produce alkalinity necessary for carbonate precipitation, we propose that vestimentifera in the southern
12 GoM largely rely on sulfide produced by sulfate-reduction coupled to methane oxidation. This is further supported by the
13 composition of the gas that forms the hydrate, which is dominated by methane (Fig. 12). The geochemistry in the southern
14 GoM is in contrast to that for vestimentifera in the northern GoM, which rely on sulfide produced by sulfate-reduction coupled
15 to methane oxidation and likely augmented by degeneration of organic carbon that may include higher hydrocarbons (e.g.,
16 Joye et al., 2004). We favor the concept that considers the vestimentifera as ecosystem engineers (sensu Cordes et al., 2003;
17 2005) that play a pivotal role for this particular gas/hydrate habitat as they intensify chemical turnover processes within the
18 rhizosphere and the space at and in between the tubes provides habitat for numerous other seep-typical species. Moreover, the
19 thick blanket of the rhizosphere shields gas hydrate from direct contact with seawater and may impede its dissolution, thereby
20 preserving the driver of AOM.

21 With regard to our discovery of the vestimentifera-gas/hydrate habitat, we attempted to characterize differences in
22 environmental parameters in the Campeche Knolls and in areas where bacterial mats drape soft sediments covering hydrates
23 (MacDonald et al., 1994; Suess et al., 2001). First, seeps in the southern GoM occur at greater water depth (~3000 m) than the
24 hydrate mounds at Hydrate Ridge (~780 m) and at Bush Hill in the northern GoM (~540 m). The higher pressure at greater
25 water depth in conjunction with very vigorous gas bubble emission, could lead to more voluminous and more rapid formation
26 of gas hydrate close to the seafloor. In addition, the deep-water physical environment is more stable compared to that at the
27 upper slope, where temperature is higher and pressure changes are considerably larger (MacDonald et al., 1994, 2005). Further,
28 with respect to the mature vestimentiferan communities and authigenic carbonates within the rhizosphere we speculate that
29 gas seepage at our study sites was stable on extended timescales: Vestimentifera are considered as long-living organisms, with
30 estimated lifespans of 170-250 years for 2 m long species in the northern GoM (Bergquist et al., 2000; Cordes et al., 2007a).
31 Although the vestimentiferan species present in the southern GoM probably belong to the genus *Escarpia* and are, thus,
32 different from those in the northern GoM, it is possible that slow growth is a general characteristic of vestimentifera at seeps
33 and that the vestimentifera observed in our study (with tube length of ~2 m) might be considerably old as well. Independent

1 support comes from a modeling study that suggested time scales of 100 to 500 years for the formation of a few cm thick
2 authigenic carbonate crust (Luff et al., 2004).

3 **5.4 Heavy oil flows leading to asphalt deposits and asphalt as habitat**

4 Our ROV-based observations revealed numerous examples for voluminous asphalt deposits at Chapopote Knoll and Mictlan
5 Knoll. Their formation has been explained by a model proposed by Brüning et al. (2010), which takes the API gravity into
6 account. Oil that floats in the water while still being attached to the seabed has an API gravity slightly higher than 10°API,
7 which corresponds to a density close to sea water. This places it at the boundary between heavy oil (10–12 to 20°API) and
8 very heavy oil (<10–12°API), that are mobile and immobile at reservoir conditions, respectively (Tissot and Welte, 1984). Oil
9 whips and sheets were observed (Fig. 7 A-C) indicating seepage of heavy oil, that is slightly positive buoyant (>10°API) but
10 sufficiently cohesive to remain attached to the point of extrusion. In contrast, the extensive asphalt deposits must have been
11 negatively buoyant (<10°API) when they exited because they clearly flowed at the seafloor (Figs. 7 D-F, Fig. 9 A).
12 Incorporation of sediments in, and accumulation of sediments onto flowing asphalts will also contribute to their negative
13 buoyancy. Formation of asphalt deposits, thus, depends on the viscosity of the extruded heavy to very heavy oil (~10°API)
14 and the duration it is exposed to weathering processes at the seafloor that lead to a transition from mobile to immobile, i.e. the
15 viscosity is high enough to allow the ascent through the sediment, but after emission at the seafloor, it rapidly becomes
16 immobile, probably due an increase in viscosity due to the loss of volatile compounds.

17 In spite of this, additional possibly post-depositional processes lead to a decrease in bulk density, which can be deduced from
18 observations at the main asphalt field at Chapopote Knoll. Pure gas hydrate, which typically exhibits a specific density less
19 than seawater (ca. 0.9 g cm⁻³), was present below and within fresh asphalts (Schubotz et al., 2011b; Klapp et al., 2010a, b) and
20 asphalt pieces floated up when extracted from an intact flow (Brüning et al., 2010). The elevated gas content might be explained
21 by post-depositional hydrate formation and gas invasion into the pore space of the asphalts resulting from gas supply from
22 below. However, with respect to the considerable difference in $\delta^{13}\text{C}$ signatures between hydrate methane below the asphalts (-
23 54.8 ‰; Schubotz et al., 2011b) and the vent gas methane (-46.5 ‰; Fig. 12) it is unlikely that these gases share the same
24 source. A possible interpretation for the more negative $\delta^{13}\text{C}$ -signature of hydrate-bound methane could be that microbial
25 methane is produced in sufficient amounts in shallow, hydrocarbon-soaked sediments below or within the asphalts.

26 As we did not observe active extrusion of heavy oil during the ROV dives, discharge rates of heavy oil at the seafloor remain
27 unknown but could, possibly, be in the range of weeks to years. The heavy oil apparently serves as energy source for
28 chemosynthesis-based organisms like whitish bacterial mats and vestimentiferan tubeworms that generally depend on the
29 supply of reduced sulfur compounds (Hilario et al., 2011; Teske & Nelson, 2006). If the outflow of heavy oil is a slow process,
30 chemosynthetic organisms may grow while the oil is still in motion. Alternatively, the chemosynthetic organism may settle
31 after deposition. Chemosynthetic organisms may thrive on reduced sulfur compounds contained in the heavy oil or on sulfide
32 produced during microbial oil degradation coupled to sulfate reduction (Schubotz et al., 2011b).

1 Based on their distribution at the seafloor exemplified in Fig. 7 D, E, we propose that predominantly relatively young ejections,
2 such as whips and sheets in the water column, and those in the central parts of asphalt flows, are populated by whitish bacterial
3 mats. Moreover, the spatial extent of bacterial mats at the main asphalt field at Chapopote Knoll during this study in 2015 was
4 very similar to that observed during its initial documentation in 2006 (Brüning et al., 2010) demonstrating considerable
5 ecosystem stability over a decade. This is remarkable as we observed holothurians, galatheid crabs, and myriads of small
6 crustaceans inferred to be grazing on the bacteria. This indicates a high primary production by chemosynthetic microbes. At
7 more distal parts of the most recent asphalt deposits, bacterial mats were absent, while tubeworms occurred nestling in fissures
8 (Fig. 7 E and Fig. 9 A). Considering the relatively low growth rates of vestimentiferan tubeworms (Bergquist et al., 2000), we
9 propose that even the most recent asphalt deposits discovered in this study already have existed for decades. The ostensible
10 absence of bacteria on asphalt surface and the presence of vestimentifera growing posteriorly into the substrate suggest that
11 the sulfide source progresses towards deeper parts of the asphalts with time. This would be in line with our concept of
12 successive stages represented by bacteria and tubeworms, respectively.

13 The most common asphalt deposits in our study were in an “inert stage”. It was devoid of any macro- or megafauna and ranged
14 in terms of appearance from solid asphalt flows to partly to entirely fragmented asphalt deposits (e.g. Fig. 9 B). We suggest
15 that these asphalts no longer serve as habitats for chemosynthesis-based bacteria or tubeworms anymore because a greater
16 portion of volatiles has already escaped to the water column. Furthermore, we point out that authigenic carbonates were
17 virtually absent where fragmented asphalts occurred alone, i.e. without oil or gas seepage (Naehr et al., 2009). This observation
18 suggests that microbial degradation of heavy oil does not produce sufficient alkalinity for authigenic carbonate formation.
19 Based on our findings we may refer to the asphalt deposits without visible chemosynthetic fauna prevailing in Campeche
20 Knolls as being in an “inert stage”. Heterotrophic suspension feeders that are common in other regions with asphalt deposits
21 (Weiland et al., 2008; Williamson et al., 2008; Valentine et al., 2010; Jones et al., 2014) were also absent on the inert stage at
22 Campeche Knolls. In our study area soft corals attached to asphalts were only found at the shallowest site investigated, UNAM
23 ridge at 1230 m water depth (Fig. 11 A). Therefore, the paucity of suspension feeders in the region of the Campeche Knolls
24 might be caused by a limited food supply at the deep-water asphalt deposits Mictlan Knoll and Chapopote Knoll (3420 to 2900
25 m water depth, respectively).

26 In contrast to seafloor asphalt deposits in other regions (Weiland et al., 2008; Williamson et al., 2008; Valentine et al., 2010;
27 Jones et al., 2014), those in the Campeche Knolls are sourced by geologically recent emissions of heavy oil. However, given
28 that lobate flow patterns are still discernible for asphalts in the Santa Barbara Basin 31 to 44 kyr after seafloor deposition
29 (Valentine et al., 2010), asphalt deposits sourced by emission of heavy oil in the Campeche Knolls may have existed for tens
30 to probably hundred thousands of years while being fragmented and draped by sediments. The Campeche Knolls asphalts
31 provide a natural laboratory to study their more recent genesis as well as their alteration through time.

1 **5.5 Oil seepage and oil-soaked sediments as habitat**

2 Because oil seepage is an integral component of the hydrocarbon seepage system at Campeche Knolls, as revealed by numerous
3 oil slicks at the sea surface (Fig. 1), we concentrated on identifying oil seepage sites at the seafloor. In general, oil may rise as
4 oil-coated gas bubbles or as oil drops (De Beukelaer et al., 2003; Leifer and MacDonald, 2003). Oily bubbles are difficult to
5 identify visually during ascent through the water column, as they can appear as transparent as pure gas bubbles. Therefore, oil
6 might have been a significant component of the observed gas bubble streams. Only in a few instances, the coating of gas
7 bubbles was dark and the hydrate forming from the bubbles was dark-stained. In contrast, release of oil drops was clearly
8 observed and occurred in association with two different seafloor manifestations: white-coated chimneys (Fig. 6 D) and oil-
9 soaked sediments inhabited by *Bathymodiolus heckeræ* (Fig. 9 F). These observations demonstrate that a seep system of oil
10 exists next to a seep system of heavy oil leading to asphalt deposits. Seepage of oil was associated with old asphalt deposits
11 (sediment-covered asphalt mounds and fragmented asphalt pieces) at three sites (Marker M114-1 and M115-5 at Mictlan
12 Knoll; bubble site at Chapopote Knoll) suggesting that the oil migrated through the sediments along preexisting pathways.
13 At Chapopote Knoll and Mictlan Knoll biological communities were physically exposed to oil (Figs. 6 F, 9 F). As found in
14 the northern GoM, degradation of oil-derived components in sediments, like non-methane hydrocarbons, can be performed by
15 sulfate-reducing bacteria (belonging to the δ -proteobacteria group) while producing hydrogen sulfide (e.g. Joye et al., 2004;
16 Kniemeyer et al., 2007). This is used as energy source for chemosynthesis-based organisms such as mat-forming, sulfide-
17 oxidizing bacteria and vestimentifera living in symbiosis with chemosynthetic bacteria. The two mytilid species studied in our
18 area harbor symbionts that are capable of oxidizing sulfides as well as methane (Raggi et al., 2013). In addition, the mussel
19 *Bathymodiolus heckeræ* from the “bubble site” at Chapopote Knoll evidenced a unique symbiosis with a proteobacterium of
20 the genus *Cycloclasticus* that is supposed to degrade hydrocarbons (Raggi et al., 2013). This symbiosis is unique to that site
21 where the animals are virtually bathed in oil.

22 **6 Summary**

23 Natural oil seepage is inherent to Campeche Knolls, as revealed by our new findings obtained during cruise M114 in 2015,
24 and by a reanalyses of seafloor images gathered during previous cruises. Unique to Campeche Knolls is the widespread
25 occurrence of asphalt deposits, which was definitely confirmed at seven sites. The flow structures of heavy oil encountered at
26 Chapopote Knoll and Mictlan Knoll are noteworthy, as they represent more recent asphalt deposits when compared to those
27 described from other continental margin settings. The recently discharged asphalts sustain chemosynthetic organisms such as
28 bacterial mats and vestimentifera as well as a suite of heterotrophic organisms that warrant further taxonomic studies. Based
29 on our preliminary observations, and in contrast to the asphalt deposits at other continental margins, those at the deeper
30 Campeche Knolls (>2900 m water depth) are generally not utilized by sessile, filter-feeding organisms that attach to hard
31 substrates.

1 Seepage of oil and gas bubbles co-occurs next to and through the asphalt deposits. Most intriguing was our finding of vigorous
2 gas bubble streams forming hydrate mounds (Tsanyao Yang Knoll) or percolating through old, fragmented asphalts leading to
3 hydrate precipitation in the voids between the asphalt breccia (Mictlan Knoll). The hydrates likely serve as shallow methane
4 reservoir underlying dense communities of vestimentiferan tubeworms, which then act as ecosystem engineers, facilitating
5 AOM and preserving the hydrate. We further suggest that in the tubeworms rhizosphere intense microbially-mediated turn-
6 over processes are probably taking place that facilitated the precipitation of authigenic carbonates. Our observation of the
7 closely associated hydrate and vestimentiferan tubeworm is unparalleled, but this relationship and the involved biogeochemical
8 processes could also be relevant in other hydrocarbon settings with shallow hydrate deposits. The healthy-appearing
9 vestimentifera growing on hydrate suggest considerable stability of these habitats over extended timespans, required for
10 establishment of the slow-growing vestimentifera and formation of authigenic carbonates.
11 Oil drops escaped the seafloor through small chimney-like structures, or, together with gas bubbles, through a mixture of
12 fragmented, old asphalt and sediments. In the latter case, sediments were heavily impregnated by oil. The seep-associated
13 communities appeared very diverse, with two chemosynthetic mussel species and various other heterotrophic organisms.

14 **Author contribution**

15 Maxim Rubin Blum, Gerhard Bohrmann, Christian Borowski, Chieh-Wei Hsu, Markus Loher, Ian MacDonald, Yann Marcon,
16 Miriam Römer, Heiko Sahling, Florence Schubotz, Daniel Smrzka, and Gunter Wegener conducted the ROV dives as scientific
17 advisors on which this present study is largely based on. Chieh-Wei Hsu, Markus Loher, and Miriam Römer detected the gas
18 emissions by hydroacoustic means. Thomas Pape analyzed the gas. Adriana Gaytán-Caballero assisted in taxonomic
19 determination of fauna at sea. Elva Escobar-Briones supported the application procedure to acquire the Mexican research
20 permission and supervised the participation of three Mexican scientists and students in the cruise. Heiko Sahling prepared the
21 manuscript with contributions of all co-authors.

22 **Acknowledgement**

23 We are grateful to the Mexican authorities for granting permission to conduct the research in the southern Gulf of Mexico
24 (permission of DGOPA: 02540/14 from 5 November 2014). We thank the master and crew of R/V *Meteor* for their highly
25 professional assistance at sea. Thanks to MARUM AUV SEAL 5000 and ROV QUEST 4000m teams for providing and
26 handling of the indispensable equipment at sea. Various people have contributed to the successful cruise, we namely thank
27 Monika Breitzke, Stefanie Buchheister, Christian Ferreira, Patrizia Geprägs, Jan-Derk Groeneveld, Elvira Jiménez
28 Guadarrama, Ingo Klaucke, Sven Klüber, Esmeralda Morales Dominguez, Gopika Suresh, Marta Torres, Monika Wiebe, Paul
29 Wintersteller, and Jennifer Zwicker. We thank three anonymous reviewer and Daniel Orange for their constructive comments
30 that improved the manuscript. The cruise was core funded by the German Research Foundation (DFG – Deutsche

1 Forschungsgemeinschaft) through the cruise proposal “Hydrocarbons in the southern Gulf of Mexico“. Additional support was
2 provided through the DFG-Research Center / Excellence Cluster “The Ocean in the Earth System”.

3 **Literature**

- 4 Bergquist, D. C., Williams, F. M., and Fisher, C. R.: Longevity record for deep-sea invertebrate, *Nature*, 403, 499-500, 2000.
- 5 Boetius, A., Ravensschlag, K., Schubert, C. J., Rickert, D., Widdel, F., Gieseke, A., Amann, R., Jørgensen, B. B., Witte, U.,
6 and Pfannkuche, O.: A marine microbial consortium apparently mediating anaerobic oxidation of methane, *Nature*, 407,
7 623-626, 2000.
- 8 Bohrmann, G. and Schenk, S.: RV *Sonne*. Cruise report SO 174, OTEGA II: (Lotus-Omega-Mumm). Balboa-Corpus Christi-
9 Miami. October 1 - November 12, 2003, 117 pp., 2004.
- 10 Bohrmann, G., Spiess, V., and cruise participants: Report and preliminary results of R/V *Meteor* Cruise M67/2a and 2b, Balboa
11 - Tampico - Bridgetown, 15 March - 24 April, 2006. Fluid seepage in the Gulf of Mexico., *Berichte Fachbereich*
12 *Geowissenschaften, Universität Bremen, Bremen*, 263, 119 pp., 2008.
- 13 Bourry, C., Chazallon, B., Charlou, J. L., Donval, J. P., Ruffine, L., Henry, P., Geli, L., and Cagatay, M. N.: Free gas and gas
14 hydrates from the Sea of Marmara, Turkey. Chemical and structural characterization, *Chemical Geology*, 264, 192-206,
15 2009.
- 16 Brüning, M., Sahling, H., MacDonald, I. R., Ding, F., and Bohrmann, G.: Origin, distribution, and alteration of asphalts at
17 Chapopote Knoll, Southern Gulf of Mexico, *Marine and Petroleum Geology*, 27, 1093-1106, 2010.
- 18 Bryant, R. B., Lugo, J., Córdova, C., and Salvador, A.: Physiography and bathymetry. In: *The Geology of Northern America,*
19 *The Gulf of Mexico Basin, Salvador, A. (Ed.), Geological Society of America, Boulder, Colorado, 1991.*
- 20 Caress, D. W. and Cheyes, D. N.: <http://www.mbari.org/data/mbsystem/>, last access: 31 January 2014, 2014.
- 21 Cordes, E. E., Bergquist, D. C., Shea, K., and Fisher, C. R.: Hydrogen sulphide demand of long-lived vestimentiferan tube
22 worm aggregations modifies the chemical environment at deep-sea hydrocarbon seeps, *Ecology Letters*, 6, 212-219, 2003.
- 23 Cordes, E. E., Bergquist, D. C., Redding, M. L., and Fisher, C. R.: Patterns of growth in cold-seep vestimentiferans including
24 *Seepiophila jonesi*: a second species of long-lived tubeworm, *Marine Ecology*, 28, 160-168, 2007a.
- 25 Cordes, E. E., Carney, S. L., Hourdez, S., Carney, R. S., Brooks, J. M., and Fisher, C. R.: Cold seeps of the deep Gulf of
26 Mexico: Community structure and biogeographic comparison to Atlantic equatorial belt seep communities, *Deep-Sea*
27 *Research I*, 54, 637-653, 2007b.
- 28 Cordes, E. E., Hourdez, S., Predmore, B. L., Redding, M. L., and Fisher, C. R.: Succession of hydrocarbon seep communities
29 associated with the long-lived foundation species *Lamellibrachia luymeri*, *Marine Ecology Progress Series*, 305, 17-29,
30 2005.
- 31 Cruz-Mercado, M. Á., Flores-Zamora, J. C., León-Ramírez, R., López-Céspedes, H. G., Peterson-Rodríguez, R. H., Reyes-
32 Tovar, E., Sánchez-Rivera, R. S., and Barrera-González, D.: Salt provinces in the Mexican portion of the Gulf of Mexico

1 - structural characterization and evolutionary model, Gulf Coast Association of Geological Societies Transactions, 61, 93-
2 103, 2011.

3 Dattagupta, S., Arthur, M. A., and Fisher, C. R.: Modification of sediment geochemistry by the hydrocarbon seep tubeworm
4 *Lamellibrachia luymesi*: A combined empirical and modeling approach, Geochimica et Cosmochimica Acta, 72, 2298-
5 2315, 2008.

6 Dattagupta, S., Miles, L. L., Barnabei, M. S., and Fisher, C. R.: The hydrocarbon seep tubeworm *Lamellibrachia luymesi*
7 primarily eliminates sulfate and hydrogen ions across its roots to conserve energy and ensure sulfide supply, The Journal
8 of Experimental Biology, 209, 3795-3805, 2006.

9 De Beukelaer, S. M., MacDonald, I. R., Guinnasso, N. L., and Murray, J. A.: Distinct side-scan sonar, RADARSAT SAR, and
10 acoustic profiler signatures of gas and oil seeps on the Gulf of Mexico slope, Geo-Marine Letters, 23, 177-186, 2003.

11 Ding, F., Spiess, V., Brüning, M., Fekete, N., Keil, H., and Bohrmann, G.: A conceptual model for hydrocarbon accumulation
12 and seepage processors around Chapopote asphalt site, southern Gulf of Mexico: From high resolution seismic point of
13 view, Journal of Geophysical Research, 113, B08404, 2008.

14 Ding, F., Spiess, V., MacDonald, I. R., Brüning, M., Fekete, N., and Bohrmann, G.: Shallow sediment deformation styles in
15 north-west Campeche Knolls, Gulf of Mexico and their controls on the occurrence of hydrocarbon seepage, Marine and
16 Petroleum Geology, 27, 959-972, 2010.

17 Formolo, M. J., Lyons, T. W., Zhang, C., Kelley, C., Sassen, R., Horita, J., and Cole, D. R.: Quantifying carbon sources in the
18 formation of authigenic carbonates at gas hydrate sites in the Gulf of Mexico, Chemical Geology, 205, 253-264, 2004.

19 Garrison, L. E. and Martin, R. G. J.: Geologic structure in the Gulf of Mexico, U. S. Government Printing Office, Washington,
20 D. C., 1-85 pp., 1973.

21 Gaytán-Caballero, A.: *Munidopsis geyeri* Pequegnat & Pequegnat, 1970 asociado al volcán de asfalto (sur del Golfo de
22 México) y su vinculación con las poblaciones del Atlántico, master thesis, Universidad Nacional Autónoma de México,
23 Mexico City, 146pp, 2009.

24 Greinert, J., Artemov, Y., Egorov, V., Debatist, M., and McGinnis, D.: 1300-m-high rising bubbles from mud volcanoes at
25 2080m in the Black Sea: Hydroacoustic characteristics and temporal variability, Earth and Planetary Science Letters, 244,
26 1-15, 2006.

27 Haeckel, M., Suess, E., Wallmann, K., and Rickert, D.: Rising methane gas bubbles form massive hydrate layers at the seafloor,
28 Geochimica et Cosmochimica Acta, 68, 4335-4345, 2004.

29 Hilario, A., Capa, M., Dahlgren, T. G., Halanych, K. M., Little, C. T., Thornhill, D. J., Verna, C., and Glover, A. G.: New
30 perspectives on the ecology and evolution of siboglinid tubeworms, PLoS One, 6, e16309, 2011.

31 Hoehler, T. M., Alperin, M. J., Albert, D. B., and Martens, C. S.: Field and laboratory studies of methane oxidation in an
32 anoxic marine sediment: evidence for methanogenic-sulfate reducer consortium, Global Biogeochemical Cycles, 8, 451-
33 463, 1994.

1 Jones, D. O. B., Walls, A., Clare, M., Fiske, M. S., Weiland, R. J., O'Brien, R., and Touzel, D. F.: Asphalt mounds and
2 associated biota on the Angolan margin, *Deep Sea Research Part I: Oceanographic Research Papers*, 94, 124-136, 2014.

3 Joye, S. B., Boetius, A., Orcutt, B. N., Montoya, J. P., Schulz, H. N., Erickson, M. J., and Lugo, S. K.: The anaerobic oxidation
4 of methane and sulfate reduction in sediments from Gulf of Mexico cold seeps, *Chemical Geology*, 205, 219-238, 2004.

5 Klapp, S. A., Bohrmann, G., Kuhs, W. F., Mangir Murshed, M., Pape, T., Klein, H., Techmer, K. S., Heeschen, K. U., and
6 Abegg, F.: Microstructures of structure I and II gas hydrates from the Gulf of Mexico, *Marine and Petroleum Geology*, 27,
7 116-125, 2010a.

8 Klapp, S. A., Murshed, M. M., Pape, T., Klein, H., Bohrmann, G., Brewer, P. G., and Kuhs, W. F.: Mixed gas hydrate structures
9 at the Chapopote Knoll, southern Gulf of Mexico, *Earth and Planetary Science Letters*, 299, 207-217, 2010b.

10 Kniemeyer, O., Musat, F., Sievert, S. M., Knittel, K., Wilkes, H., Blumenberg, M., Michaelis, W., Classen, A., Bolm, C., Joye,
11 S. B., and Widdel, F.: Anaerobic oxidation of short-chain hydrocarbons by marine sulphate-reducing bacteria, *Nature*, 449,
12 898-902, 2007.

13 Leifer, I. and MacDonald, I.: Dynamics of the gas flux from shallow gas hydrate deposits: interaction between oily hydrate
14 bubbles and the oceanic environment, *Earth and Planetary Science Letters*, 210, 411-424, 2003.

15 Leythaeuser, D., Schaefer, R.G., and Yukler, A.: Diffusion of light hydrocarbons through near-surface rocks, *Nature*, 284,
16 522-525, 1980.

17 Luff, R., Wallmann, K., and Aloisi, G.: Numerical modeling of carbonate crust formation at cold vent sites: Significance for
18 fluid and methane budgets and chemosynthetic biological communities, *Earth and Planetary Science Letters*, 221, 337-353,
19 2004.

20 MacDonald, I., Bender, L., Vardaro, M., Bernard, B., and Brooks, J.: Thermal and visual time-series at a seafloor gas hydrate
21 deposit on the Gulf of Mexico slope, *Earth and Planetary Science Letters*, 233, 45-59, 2005.

22 MacDonald, I. R., Bohrmann, G., Escobar, E., Abegg, F., Blanchon, P., Blinova, V., Brückmann, W., Drews, M., Eisenhauer,
23 A., Han, X., Heeschen, K., Meier, F., Mortera, C., Naehr, T., Orcutt, B., Bernard, B., Brooks, J., and de Farágo, M.: Asphalt
24 volcanism and chemosynthetic life in the Campeche Knolls, Gulf of Mexico, *Science*, 304, 999-1002, 2004.

25 MacDonald, I. R., Escobar, E., Naehr, T., Joye, S., and Spiess, V.: The asphalt ecosystem of the Gulf of Mexico: Results from
26 the Chapopte III Cruise, Fall Meet. Suppl., Abstract B43E-1660, 2007.

27 MacDonald, I. R., Garcia-Pineda, O., Beet, A., Daneshgar Asl, S., Feng, L., Graettinger, G., French-McCay, D., Holmes, J.,
28 Hu, C., Huffer, F., Leifer, I., Muller-Karger, F., Solow, A., Silva, M., and Swayze, G.: Natural and unnatural oil slicks in
29 the Gulf of Mexico, *Journal of Geophysical Research: Oceans*, 120, 8364-8380, 2015.

30 MacDonald, I. R., Guinasso jr., N. L., Ackleson, S. G., Amos, J. F., R., D., Sassen, R., and Brooks, J. M.: Natural oil slicks in
31 the Gulf of Mexico visible from space, *Journal of Geophysical Research*, 98, 16351-16364, 1993.

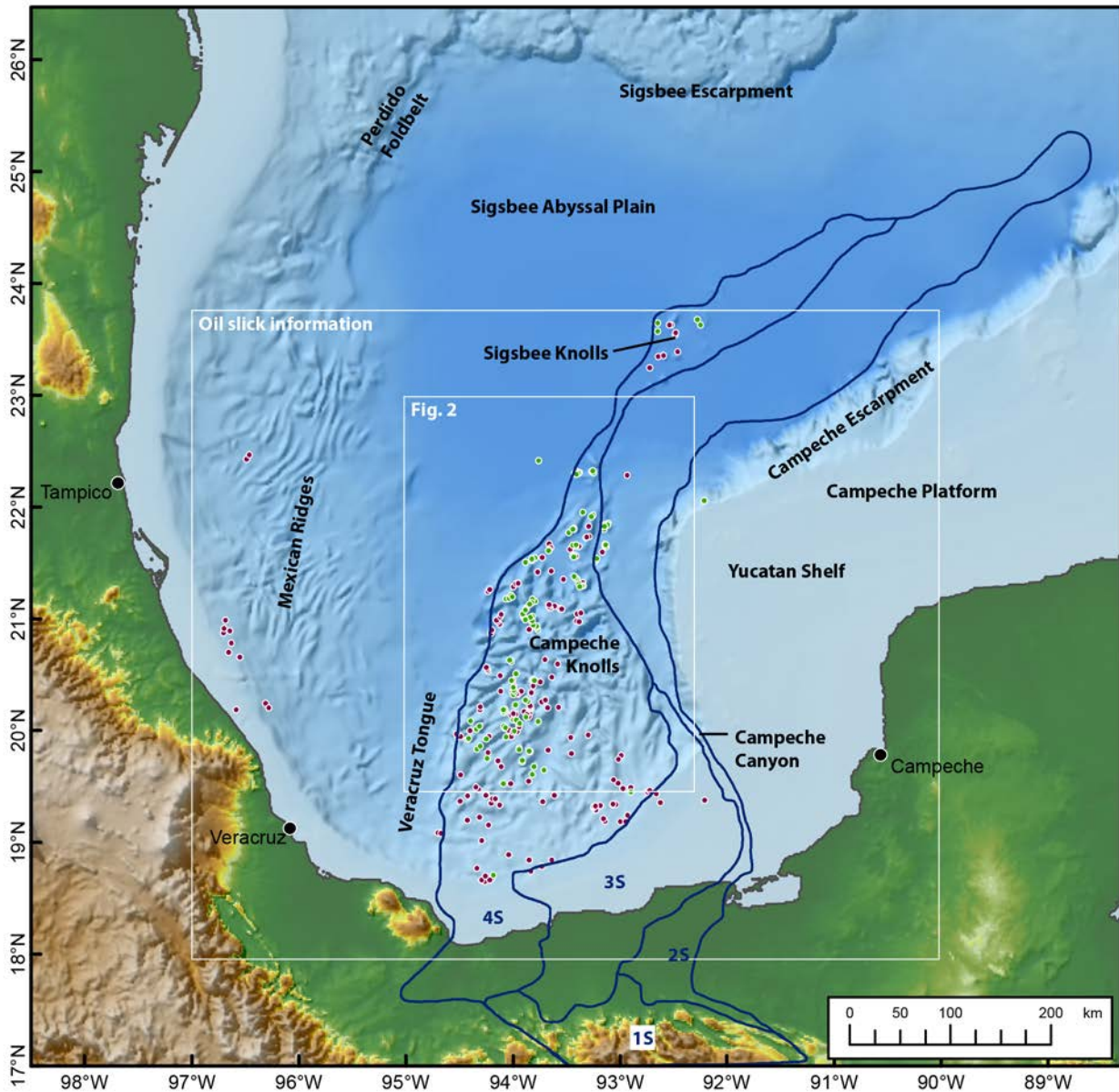
32 MacDonald, I. R., N. L. Guinasso, J., Sassen, R., Brooks, J. M., Lee, L., and Scott, K. T.: Gas hydrate that breaches the sea
33 floor on the continental slope of the Gulf of Mexico, *Geology*, 22, 699-702, 1994.

- 1 MacDonald, I. R., Reilly, J. F., Jr., Best, S. E., Venkataramaiah, R., Sassen, R., and Guinasso, N. L., Jr.: Remote sensing
2 inventory of active oil seeps and chemosynthetic communities in the northern Gulf of Mexico. In: Hydrocarbon migration
3 and its near-surface expression, Schumacher, D. and Abrams, M. A. (Eds.), American Association of Petroleum Geologists,
4 27-37, 1996.
- 5 Magoon, L. B., Hudson, T. L., and Cook, H. E.: Pimienta-Tamabra (!) - A giant supercharged petroleum system in the southern
6 Gulf of Mexico, onshore and offshore Mexico. In: The western Gulf of Mexico basin: Tectonics, sedimentary basins, and
7 petroleum systems, Bartolini, C., Biuffler, R. T., and Cantú-Chapa, A. (Eds.), AAPG Memoir, 75, 83-125, 2001.
- 8 Milkov, A.V. and Dzou, L.: Geochemical evidence of secondary microbial methane from very slight biodegradation of
9 undersaturated oils in a deep hot reservoir, *Geology*, 35, 455-458, 2007.
- 10 Naehr, T. H., Birgel, D., Bohrmann, G., MacDonald, I. R., and Kasten, S.: Biogeochemical controls on authigenic carbonate
11 formation at the Chapopote “asphalt volcano”, Bay of Campeche, *Chemical Geology*, 266, 390-402, 2009.
- 12 Nikolovska, A., Sahling, H., and Bohrmann, G.: Hydroacoustic methodology for detection, localization, and quantification of
13 gas bubbles rising from the seafloor at gas seeps from the Black Sea, *Geochemistry Geophysics Geosystems*, 9, Q10010,
14 2008.
- 15 Pape, T., Bahr, A., Rethemeyer, J., Kessler, J. D., Sahling, H., Hinrichs, K.-U., Klapp, S. A., Reeburgh, W. S., and Bohrmann,
16 G.: Molecular and isotopic partitioning of low-molecular-weight hydrocarbons during migration and gas hydrate
17 precipitation in deposits of a high-flux seepage site, *Chemical Geology*, 269, 350-363, 2010.
- 18 Paull, C. K., Hecker, B., Commeau, R., Freeman-Lynde, R. P., Neumann, C., Corso, W. P., Golubic, S., Hook, J. E., Sikes, E.,
19 and Curray, J.: Biological communities at the Florida Escarpment resemble hydrothermal vent taxa, *Science*, 226, 965-
20 967, 1984.
- 21 Raggi, L., Schubotz, F., Hinrichs, K. U., Dubilier, N., and Petersen, J. M.: Bacterial symbionts of *Bathymodiolus* mussels and
22 *Escarpia* tubeworms from Chapopote, an asphalt seep in the southern Gulf of Mexico, *Environmental Microbiology*, 15,
23 1969-1987, 2013.
- 24 Roberts, H. H., Shedd, W., and Hunt Jr, J.: Dive site geology: DSV ALVIN (2006) and ROV JASON II (2007) dives to the
25 middle-lower continental slope, northern Gulf of Mexico, *Deep Sea Research Part II: Topical Studies in Oceanography*,
26 57, 1837-1858, 2010.
- 27 Römer, M., Sahling, H., Pape, T., Bahr, A., Feseker, T., Wintersteller, P., and Bohrmann, G.: Geological control and magnitude
28 of methane ebullition from a high-flux seep area in the Black Sea-the Kerch seep area, *Marine Geology*, 319-322, 57-74,
29 2012.
- 30 Sahling, H., Rickert, D., Lee, R. W., Linke, P., and Suess, E.: Macrofaunal community structure and sulfide flux at gas hydrate
31 deposits from the Cascadia convergent margin, NE Pacific, *Marine Ecology Progress Series*, 231, 121-138, 2002.
- 32 Salvador, A. (Ed.): The Gulf of Mexico basin, *Geology of North America*, Geological Society of America, Boulder, Colorado,
33 568p, 1991.

- 1 Sánchez-Rivera, R. S., Cruz-Mercado, M. Á., Reyes-Tovar, E., López-Céspedes, H. G., Peterson-Rodriguez, R. H., Flores-
2 Zamora, J. C., Ramirez, R. L., and Barrera-González, D.: Tectonic evolution of the South Gulf Salt Province in the Gulf of
3 Mexico, Gulf Coast Association of Geological Societies Transactions, 61, 421-427, 2011.
- 4 Sassen, R., Roberts, H. H., Carney, R., Milkov, A. V., DeFreitas, D. A., Lanoil, B., and Zhang, C.: Free hydrocarbon gas, gas
5 hydrate, and authigenic minerals in chemosynthetic communities of the northern Gulf of Mexico continental slope: relation
6 to microbial processes, Chemical Geology, 205, 195-217, 2004.
- 7 Scholz-Böttcher, B. M., Ahlf, S., Vazquez-Gutierrez, F., and Rullkötter, J.: Sources of hydrocarbon pollution in surface
8 sediments of the Campeche Sound, Gulf of Mexico, revealed by biomarker analysis, Organic Geochemistry, 39, 1104-
9 1108, 2008.
- 10 Schubotz, F., Lipp, J. S., Elvert, M., and Hinrichs, K.-U.: Stable carbon isotopic compositions of intact polar lipids reveal
11 complex carbon flow patterns among hydrocarbon degrading microbial communities at the Chapopote asphalt volcano,
12 Geochimica et Cosmochimica Acta, 75, 4399-4415, 2011a.
- 13 Schubotz, F., Lipp, J. S., Elvert, M., Kasten, S., Mollar, X. P., Zabel, M., Bohrmann, G., and Hinrichs, K.-U.: Petroleum
14 degradation and associated microbial signatures at the Chapopote asphalt volcano, Southern Gulf of Mexico, Geochimica
15 et Cosmochimica Acta, 75, 4377-4398, 2011b.
- 16 Smith, A. J., Flemings, P. B., Liu, X., and Darnell, K.: The evolution of methane vents that pierce the hydrate stability zone in
17 the world's oceans, Journal of Geophysical Research: Solid Earth, 119, 6337-6356, 2014.
- 18 Suess, E., Torres, M. E., Bohrmann, G., Collier, R. W., Rickert, D., Goldfinger, C., Linke, P., Heuser, A., Sahling, H.,
19 Heeschen, K., Jung, C., Nakamura, K., Greinert, J., Pfannkuche, O., Trehu, A., Klinkhammer, G., Whiticar, M. J.,
20 Eisenhauer, A., Teichert, B., and Elvert, M.: Sea floor methane hydrates at Hydrate Ridge, Cascadia Margin. In: Natural
21 gas hydrates: Occurrence, distribution, and detection, Paull, C. (Ed.), Geophysical Monograph 124, American Geophysical
22 Union, 87-98, 2001.
- 23 Suresh, G.: Offshore oil seepage visible from space: A Synthetic Aperture Radar (SAR) based automatic detection, mapping
24 and quantification system, Dissertation Thesis, Department of Geosciences, University of Bremen, 180p, 2015.
- 25 Teske, A. and Nelson, B. W.: The genera *Beggiatoa* and *Thioploca*, Prokaryotes, 6, 784-810, 2006.
- 26 Tissot, B. P. and Welte, D. H.: Petroleum formation and occurrence, Springer, Berlin, 699p, 1984.
- 27 Torres, M. E., Wallmann, K., Tréhu, A. M., Bohrmann, G., Borowski, W. S., and Tomaru, H.: Gas hydrate growth, methane
28 transport, and chloride enrichment at the southern summit of Hydrate Ridge, Cascadia margin off Oregon, Earth and
29 Planetary Science Letters, 226, 225-241, 2004.
- 30 Treude, T., Boetius, A., Knittel, K., Wallmann, K., and Jorgensen, B. B.: Anaerobic oxidation of methane above gas hydrates
31 at Hydrate Ridge, NE Pacific Ocean, Marine Ecology Progress Series, 264, 1-14, 2003.
- 32 Valentine, D. L., Reddy, C. M., Farwell, C., Hill, T. M., Pizarro, O., Yoerger, D. R., Camilli, R., Nelson, R. K., Peacock, E.
33 E., Bagby, S. C., Clarke, B. A., Roman, C. N., and Soloway, M.: Asphalt volcanoes as a potential source of methane to late
34 Pleistocene coastal waters, Nature Geoscience, 3, 345-348, 2010.

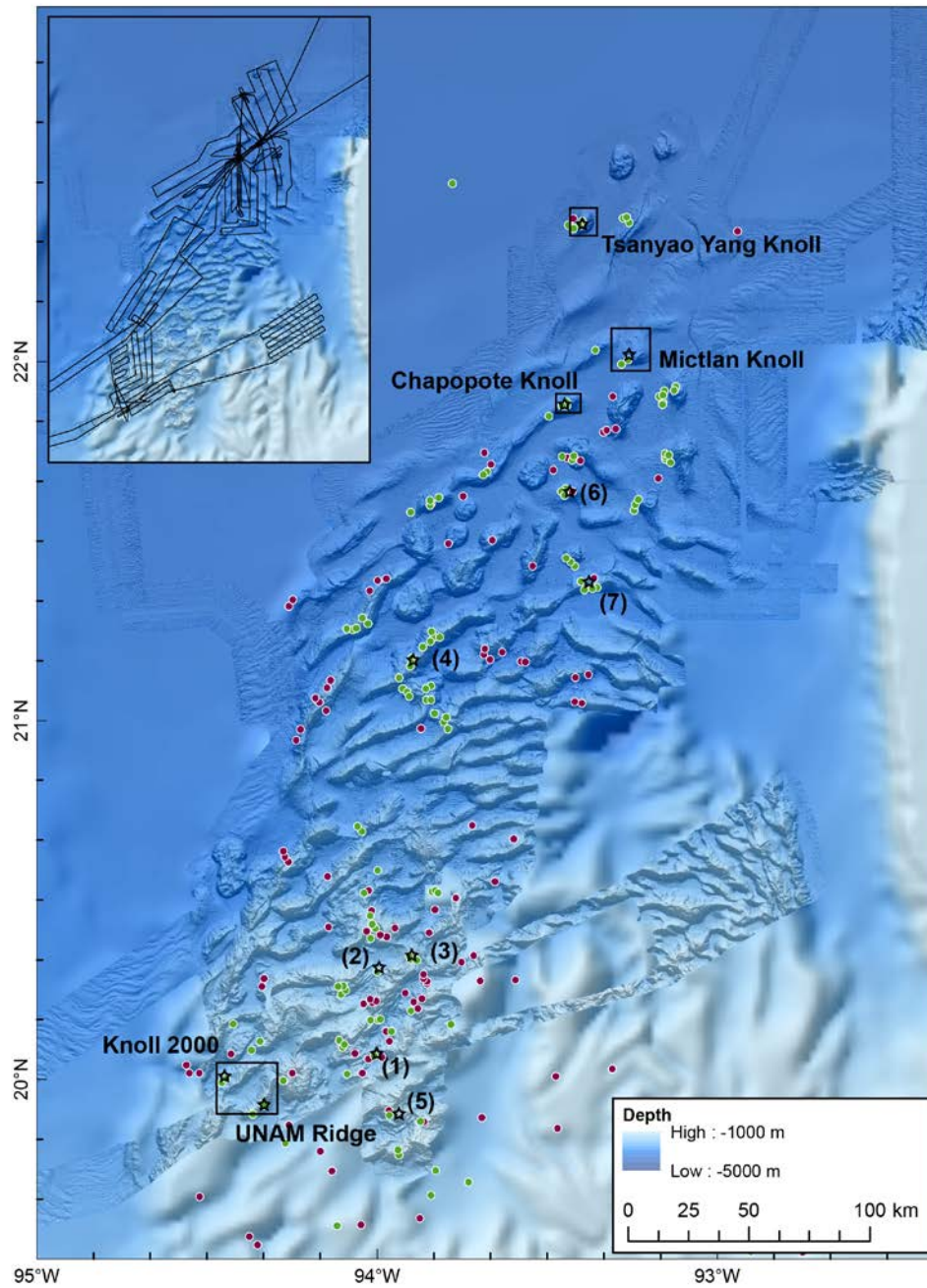
- 1 Vernon, J. W. and Slater, R. A.: Submarine tar mounds, Santa Barbara County, California, Bulletin of the American
2 Association of Petroleum Geologists, 47, 1624-1627, 1963.
- 3 Weiland, R. J., Adams, G. P., McDonald, R. D., Rooney, T. C., and Wills, L. M.: Geological and biological relationships in
4 the Puma appraisal area: From salt diapirism to chemosynthetic communities, Offshore Technology Conference, Houston,
5 Texas, USA, 5-8 May 2008, OTC-19360-PP, 2008.
- 6 Whiticar, M. J.: A geochemical perspective of natural gas and atmospheric methane, Organic Geochemistry, 16, 531-547, 1990.
- 7 Williams, A. K., Lawrence, G. M., and King, M.: Exploring for deepwater petroleum systems with satellite SAR (Synthetic
8 Aperture RADAR). Fact or Fiction? Comparing results from two of today's hotspots (Congo and Santos) with two of
9 tomorrow's (Campeche and Cariaco) (2 Poster), Adapted from poster presentation of the AAPG Annual Convention,
10 Houston, 2006 (available online: <http://www.searchanddiscovery.com/documents/2006/06100williams/index.htm>).
- 11 Williamson, S. C., Zois, N., and Hewitt, A. T.: Integrated site investigation of seafloor features and associated fauna, Shenzi
12 field, deepwater Gulf of Mexico, Offshore Technology Conference, Houston, Texas, USA, 5-8 May 2008, OTC 19356,
13 2008.
- 14

1 **Figures**



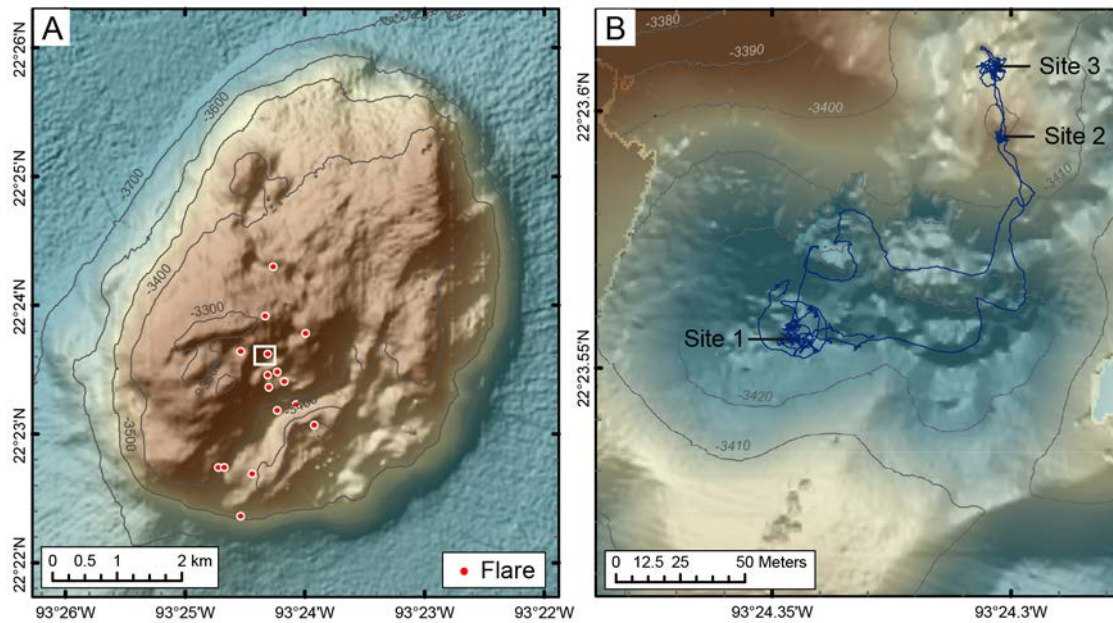
2

3 **Figure 1.** Geomorphological setting of the southern Gulf of Mexico based on shaded GEBCO bathymetry. Campeche Knolls
4 and Sigsbee Knolls are located within the sub-province 4S, which is part of the South Gulf Salt Province (outlined in blue) as
5 suggested by Cruz-Mercado et al. (2011). Locations of definite (green dots) and probable (purple dots) oil slick origins at the
6 sea surface according to Williams et al. (2006) and the extent of the respective study area (outer rectangle) are shown.



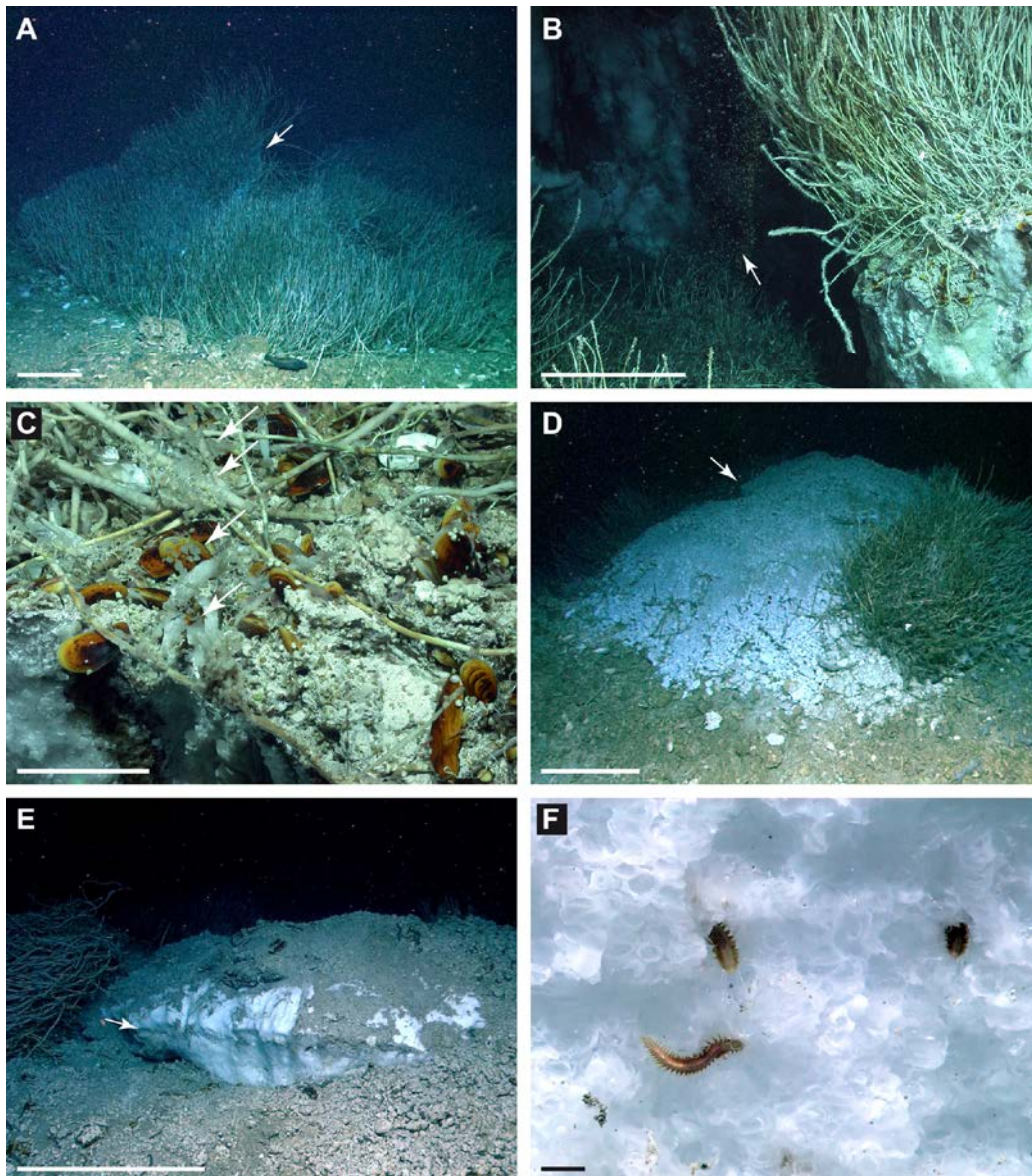
1
 2 **Figure 2.** Swath bathymetry draped over GEBCO bathymetry of the Campeche Knolls and cruise track of M 114 (inset).
 3 Indicated are oil slick origins as inferred from oil slicks at the sea surface according to Williams et al. (2006) classified as
 4 definite (green dots) and probable (purple dots). Seafloor locations of hydrocarbon seepage sites investigated in this study are
 5 also shown (open stars, number in brackets). Specifics of those sites are given in Table 1.

1
2

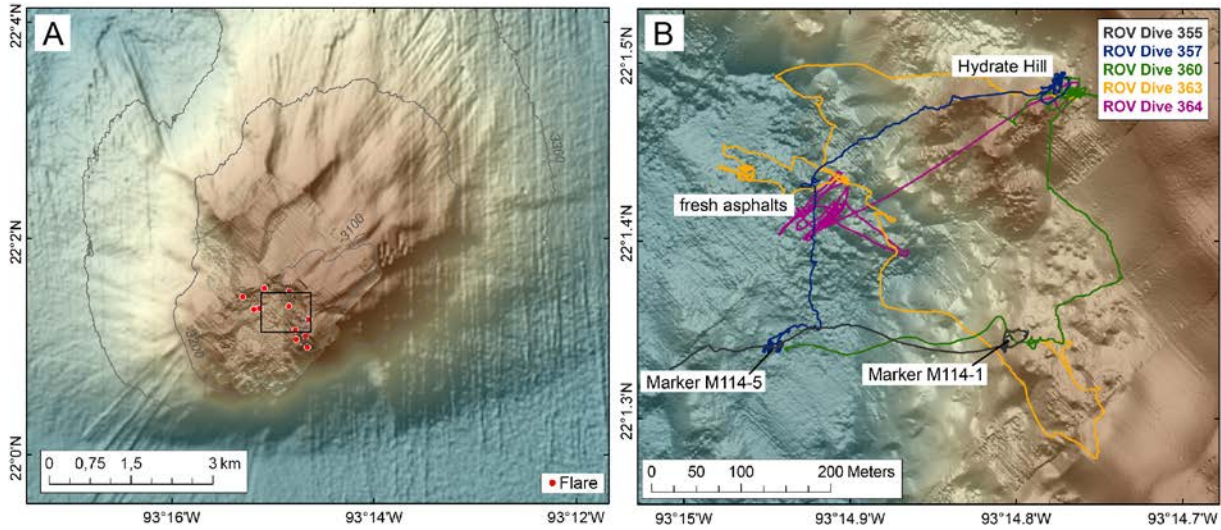


3
4

5 **Figure 3.** (A) Ship-based swath bathymetry of Tsanyao Yang Knoll (see Fig. 2 for location), flare locations (red dots), and the
6 area shown in (B) (box). (B) ROV QUEST Dive 361 track and the main study sites plotted on AUV swath bathymetry.

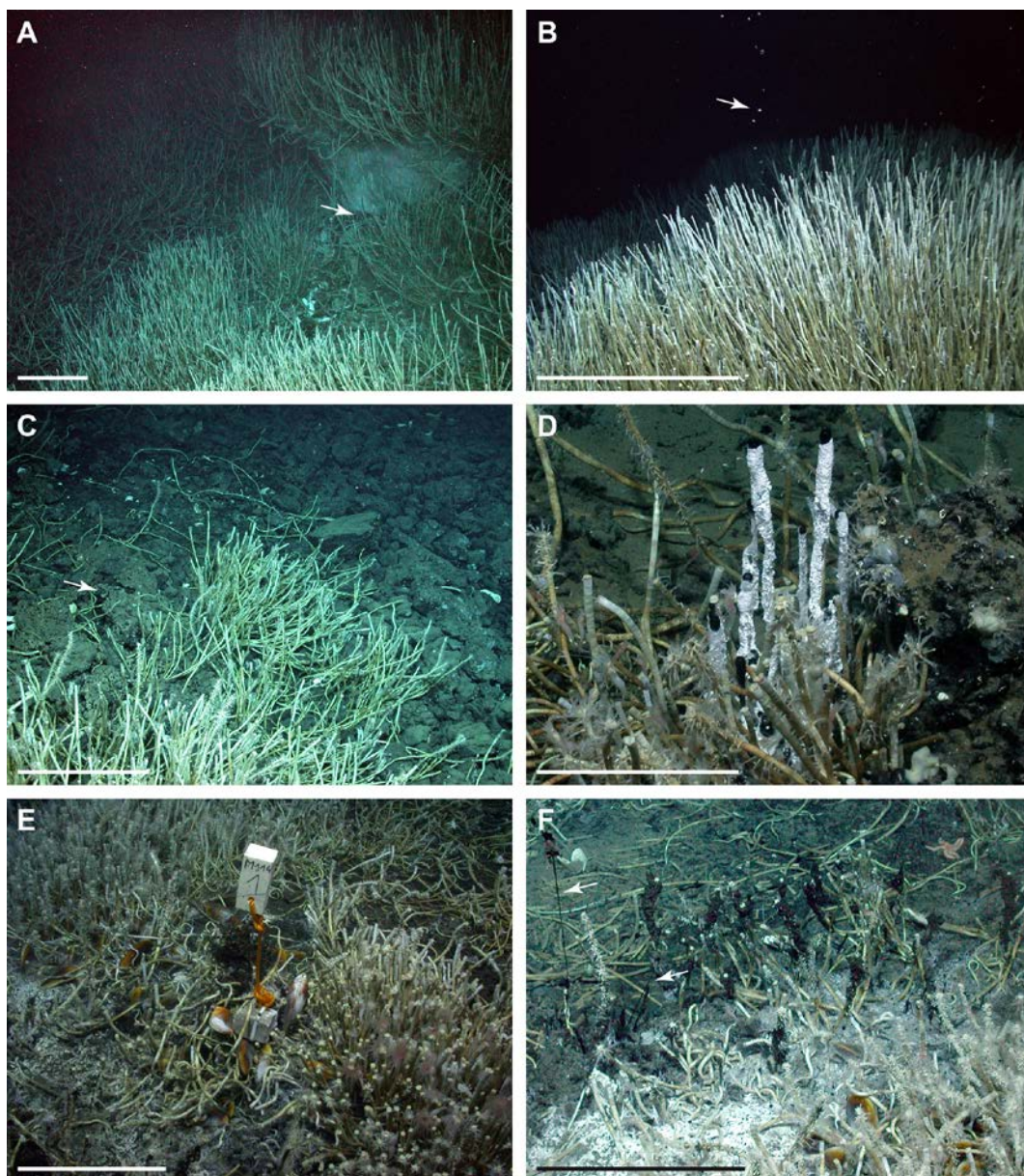


1
 2 **Figure 4.** Seafloor images taken at Tsanyao Yang Knoll during ROV QUEST Dive 361. (A) Vestimentiferan tubeworm bushes
 3 on a fractured mound (arrow). Scale bar 50 cm in foreground. (B) Gas bubble plume (arrow) rose through the gap of a fractured
 4 mound. Hydrates formed at the hanging walls. Scale bar 50 cm. (C) Close-up of the mound surface with bubbles emitted into
 5 the water column (arrows) from the same spot. Gas hydrate occurred below a layer of authigenic carbonates with mytilids,
 6 vestimentifera, gastropods, and shrimps on top. Scale bar 10 cm. (D) Mound with exposed gas hydrate (arrow) detailed in (E,
 7 F). Scale bar 50 cm. (E) Lens-shaped, exposed gas hydrate composed of bubble-fabric hydrate below and dense hydrate above
 8 the arrow. Scale bar 50 cm. (F) Bubble-fabric hydrate inhabited by ice worms (cf. *Hesiocaeca methanicola*). Scale bar 1 cm.
 9 All images courtesy of MARUM.



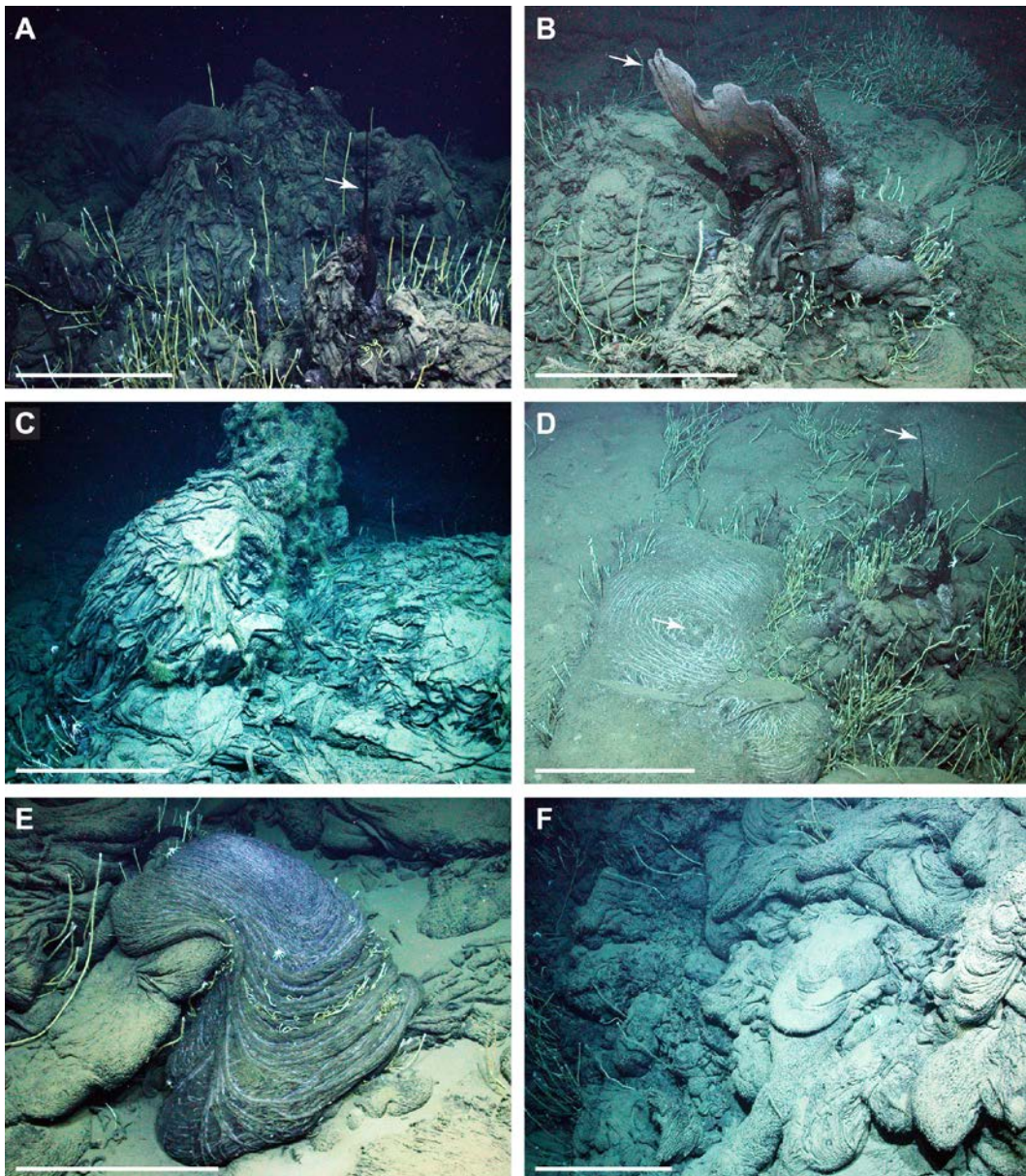
1
2
3
4
5

Figure 5. Maps of Mictlan Knoll (see Fig. 2 for location): (A) AUV-based bathymetry draped over ship-based bathymetry and positions of flares (red dots). The box defines the area illustrated in (B). (B) ROV QUEST dive tracks and main study sites plotted on AUV-based bathymetry.



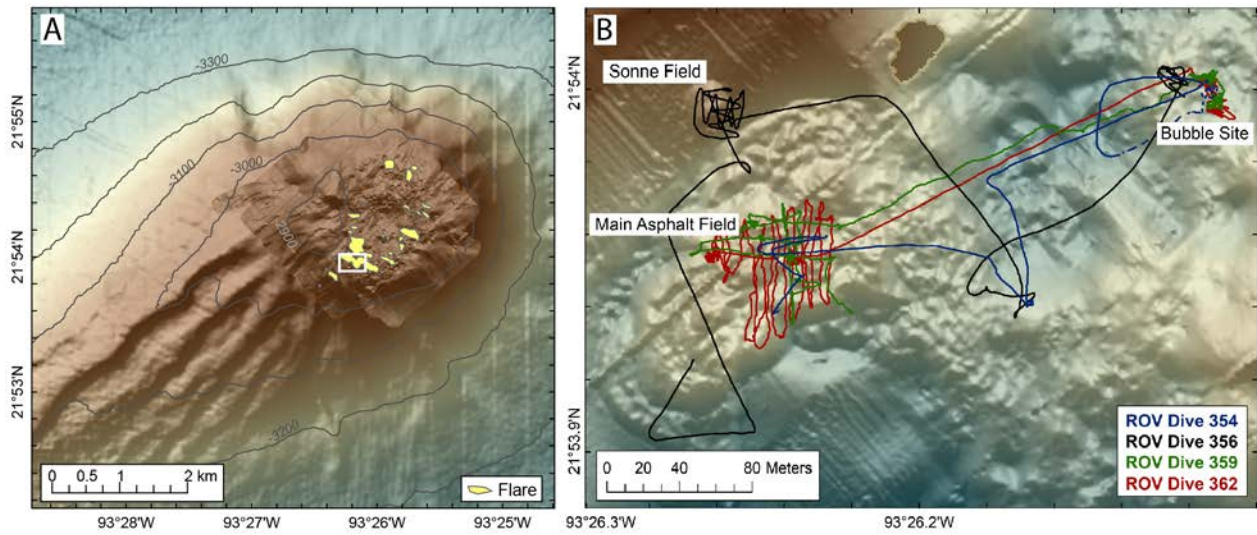
2

3 **Figure 6.** Seafloor images taken at Mictlan Knoll during ROV QUEST Dives 357 (A-D) and 360 (E-F). (A) Hydrate below
 4 overhanging vestimentiferan tubeworms (arrow). Scale bar 50 cm. (B) Gas bubble stream (arrow) rose through the hydrates
 5 and vestimentifera shown in (A). Scale bar 50 cm. (C) Fragmented asphalt, authigenic carbonates (arrow), and vestimentifera.
 6 Scale bar 50 cm. (D) Oil drops released through white-coated chimneys. Scale bar 20 cm. (E) Flourishing ecosystem (mytilids,
 7 vestimentifera with epizoic suspension feeders, bacterial mats) next to oil-soaked sediments shown in (F). (F) Viscous oil
 8 drops emanated from the sediments leaving strands behind (arrow). Scale bar 20 cm. All images courtesy of MARUM.



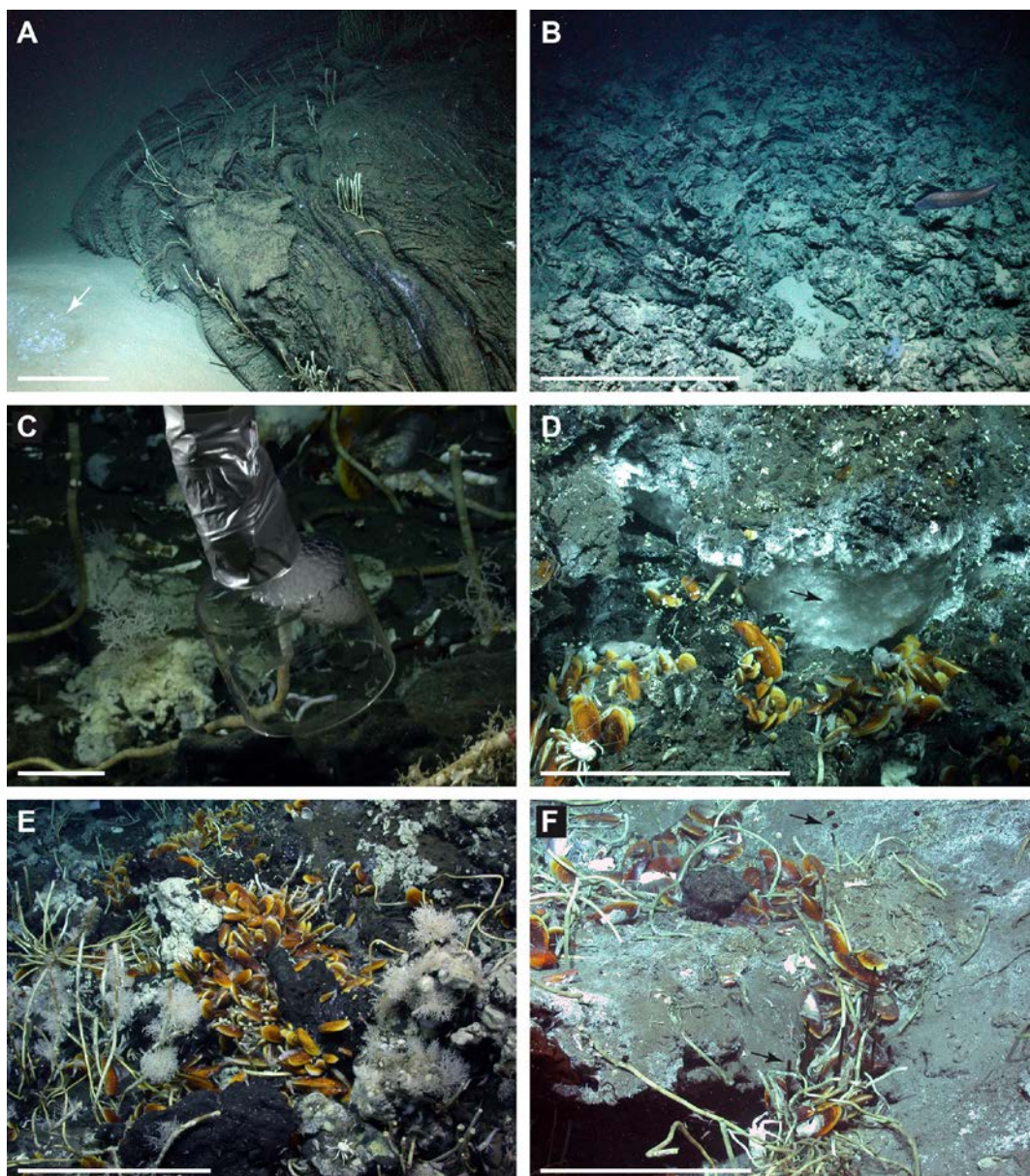
1
2
3
4
5

Figure 7. Seafloor images taken at Mictlan Knoll during ROV QUEST Dives 357 (B, C), 363 (A, E), and 364 (D-F). (A-C) Oil whips and sheets (arrows) floating in the water. Old whips and sheets apparently lost buoyancy and pile-up at the seafloor. (D-F) Flow structures of heavy oil. Scale bar all images 50 cm. All images courtesy of MARUM.



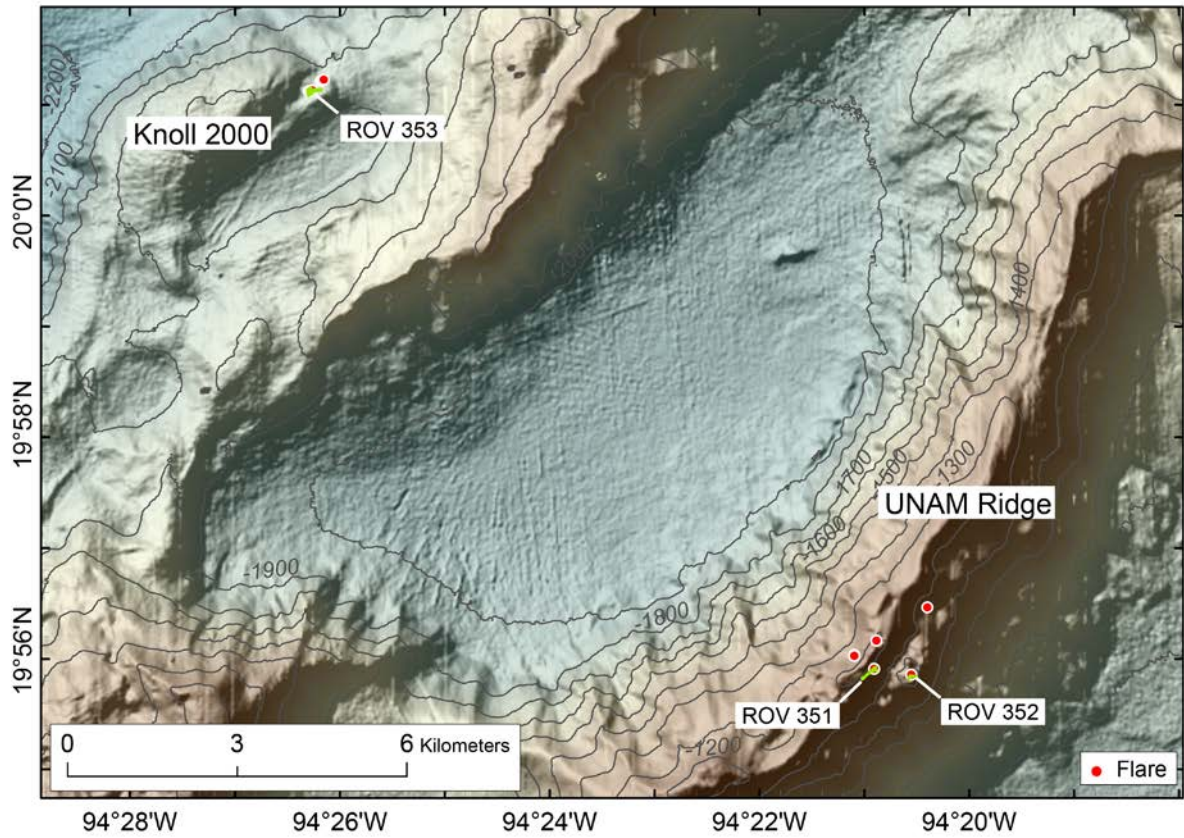
1
2
3
4
5

Figure 8. Maps of Chapopote Knoll (see Fig. 2 for location): (A) AUV-based bathymetry draped over ship-based bathymetry and areas of flares (yellow). The box shows the area in (B). (B) ROV QUEST dive tracks and main study sites plotted on AUV-based bathymetry.



2

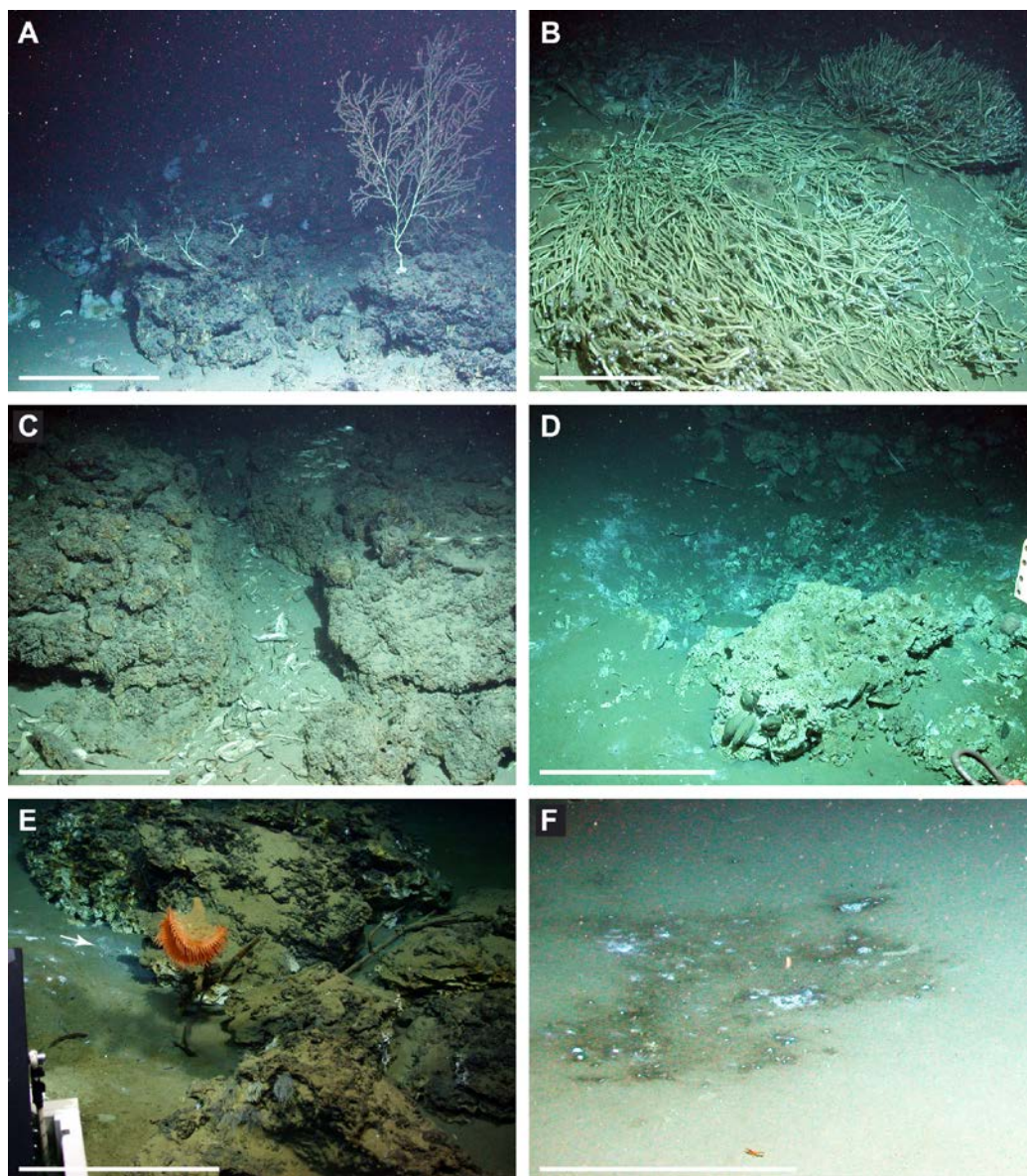
3 **Figure 9.** Seafloor images taken at Chapopote Knoll during ROV QUEST Dives 354 (C, E), 362 (A, F), and 365 (B, D). (A)
 4 Main asphalt field with vestimentifera bordering a bacterial mat (arrow) on soft sediments. Scale bar 50 cm. (B) Older flow
 5 characterized by fragmented asphalt. Scale bar 50 cm. (C) Catching hydrate-coated bubbles at the bubble site. Scale bar 10
 6 cm. (D) Gas hydrate outcrop (arrow) with mytilids, gastropods, galatheid crab. Note bubble fabric of exposed hydrate. Scale
 7 bar 50 cm. (E) Sponges, hydrozoans, mytilids at the bubble site. Scale bar 50 cm. (F) Oil drops and oil whips (arrows)
 8 close to the bubble site. Scale bar 50 cm. All images courtesy of MARUM.



1

2 **Figure 10.** Ship-based bathymetry of Knoll 2000 and UNAM Ridge (see Fig. 2 for location), locations of flares (red dots) and
3 ROV QUEST dive tracks (green).

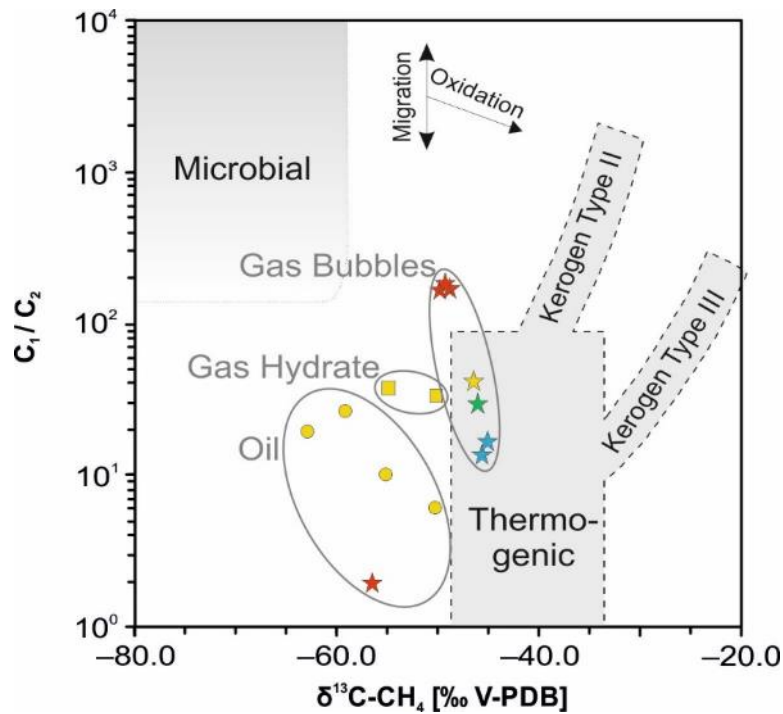
4



2

3 **Figure 11.** Seafloor images taken at UNAM Ridge (A-D) and Knoll 2000 (E-F) during ROV QUEST dives 352 and 353,
 4 respectively. (A) Soft coral and other suspension feeders on iron/manganese-stained authigenic carbonates. (B) Recumbent
 5 vestimentifera. (C) Authigenic carbonates and mytilid shells. (D) A few living mytilids attached to carbonates (foreground)
 6 and a 1 m wide circular depression. (E) Frenulate tubeworms were recovered from samples of whitish-stained sediments
 7 (arrow) next to carbonates inhabited by suspension feeders (*Actinoscyphia* sp., anemones, sponges). (F) Whitish patches at
 8 seafloor interpreted to by bacterial mats on dark-stained sediments. Scale bar all images 50 cm. All images courtesy of
 9 MARUM.

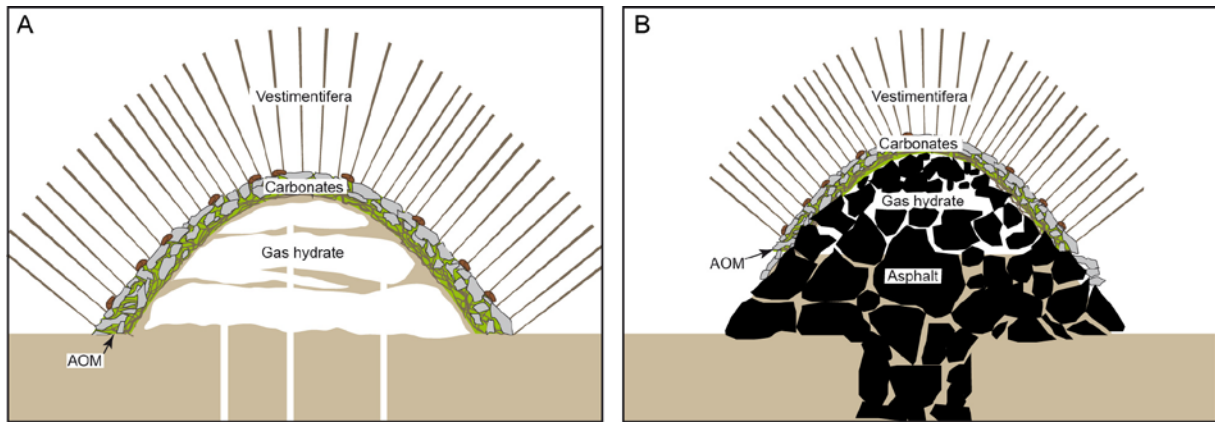
1
2
3



4
5
6
7
8
9
10

Figure 12. Molecular (C_1/C_2) vs. stable C isotopic composition of methane ($\delta^{13}C-CH_4$) sampled by Gas Bubble Sampler at Tsanyao Yang Knoll (blue), Mictlan Knoll (red), Chapopote Knoll (yellow), and UNAM Ridge (green) and a single oil-associated gas sample (Mictlan Knoll) collected during this study with the GBS. Stars indicate samples analyzed in this study, dots and squares are values according to results for methane in hydrates and oil collected during previous campaigns (MacDonald et al., 2004; Schubotz et al., 2011b). Classification according to the “Bernard diagram” modified after Whiticar (1990). Gas samples studied herein are plotted close to the empirical field of thermogenic methane.

1



2

3 **Figure 13.** Sketch depicting the interpreted vestimentifera-gas/hydrate habitat encountered at (A) Tsanyao Yang Knoll and
4 (B) Mictlan Knoll. Drawing not to scale. The mounds at Tsanyao Yang Knoll were a few meters wide whereas Hydrate Hill
5 at Mictlan Knoll was about 30 m in diameter. AOM = anaerobic oxidation of methane (green).
6

1 Tables

2 **Table 1.** Summary of evidence for hydrocarbon seepage in the southern Gulf of Mexico based on AUV SEAL 5000, ROV
 3 QUEST 4000m, and camera-sled observations obtained during cruises R/V *Sonne* cruise 174, R/V *Meteor* cruise 67/2, R/V
 4 *Justo Sierra* cruise Campeche III, and R/V *Meteor* cruise 114/2. The positions marked with an asterisk are based on ship
 5 positions.

6

| Seafloor Structure | Location | Depth | Tools | Observation |
|--------------------|----------------|--------|---|---|
| Tsanyao | 22°23.55'N; | 3420 m | M 114/2 ROV Dive 358 (15 Mar 2015), | Vestimentifera on hydrate outcrops, gas bubble |
| Yang | 93°24.33'W | | Dive 361 (19 Mar 2015), AUV Dive 69 | and oil emission, carbonates, mytilid and |
| Knoll | | | (24 Feb 2015) | vesicomimid bivalves |
| Mictlan | 22°1.4'N; | 3180 m | M 114/2 ROV Dive 355 (11 Mar 2015), | Asphalt deposits, gas bubble and oil emission, |
| Knoll | 93°14.9'W | | Dive 357 (14 Mar 2015), Dive 360 (18 | vestimentifera, white bacterial mats, mytilid and |
| | | | Mar 2015), Dive 363 (21 Mar 2015), | vesicomimid bivalves |
| | | | Dive 364 (22 Mar 2015), AUV Dive 68 | |
| | | | (23 Feb 2015) | |
| Chapopote | 21°53.95'N; | 2920 m | SO 174 OFOS 13 (01 Nov 2003), OFOS | Asphalt deposits, gas bubble and oil emission, |
| Knoll | 93°26.25'W | | 14 (02 Nov 2013); M 67/2 ROV Dive | vestimentifera, white bacterial mats, mytilid and |
| | | | 80 (10 Apr 2006), Dive 81 (11 Apr | vesicomimid bivalves |
| | | | 2006), Dive 82 (12 Apr 2016), Dive 83 | |
| | | | (14 Apr 2006), Dive 84 (15 Apr 2006); | |
| | | | M 114/2 ROV Dive 354 (10 Mar 2015), | |
| | | | Dive 356 (13 Mar 2015), Dive 359 16 | |
| | | | Mar 2015), Dive 363 (21 Mar 2015), | |
| | | | AUV Dive 70 (25 Feb 2015) | |
| UNAM | 19°55.90'N; | 1230 m | M 114/2 ROV Dive 351 (04 Mar 2015), | Asphalt deposits, carbonates, vestimentifera, |
| Ridge | 94°20.89'W | | Dive 352 (05 Mar 2015) | mytilids, gas bubble emission |
| Knoll 2000 | 20°01.12'N; | 1860 m | M114/2 ROV Dive 353 (08 Mar 2015) | Carbonates and possibly asphalts, white |
| | 94°26.20'W | | | bacterial mats on blackish seafloor, |
| | | | | pogonophoran tubeworms |
| 1 | 20°4.95'N93°57 | 1300 m | R/V <i>Justo Sierra</i> camera survey, Site | Asphalt, vestimentifera, soft coral |
| | .85'W* | | L89 (18 Sep 2007) | |
| 2 | 20°19.55'N; | 1780 m | R/V <i>Justo Sierra</i> camera survey, Site | Asphalt or carbonate pieces, sparse bacterial |
| | 93°59.15'W* | | L87 (20 Sep 2007) | mats |
| 3 | 20°22.02'N; | 1700 m | R/V <i>Justo Sierra</i> camera survey, Site | Asphalt, tubeworm, mussels |
| | 93°54.28'W* | | L86 (21 Sep 2007) | |
| 4 | 21°11.45'N; | 2335 m | R/V <i>Justo Sierra</i> camera survey, Site | Asphalt or carbonate |
| | 93°53.40'W* | | L97 (22 Sep 2007) | |
| 5 | 19°54.917'N; | 1100 m | R/V <i>Justo Sierra</i> camera survey, Site | Asphalt or carbonate, bacterial mats |
| | 93°56.366'W* | | L94 (19 Sep 2007) | |

| | | | | |
|---|--|-------------|--|--|
| 6 | 21°39.5'N; 93°26.1'W* | 2980 m | M 67/2 TV-Sled survey (09 Apr 2006) | Asphalt deposits some ten meters in diameter |
| 7 | Ca. 21°25'N; 93°22'W* and 21°23.8'N; 93°23.3'W* | 2400-2440 m | SO 174/2 OFOS 10 (29 Oct 2003), OFOS 12 (31 Oct 2003) | Sediment covered, outcropping asphalts, scattered living vesicomid clams, vestimentifera, bacterial mats |

1